January 2015

Smarcb1-Mutant Intracranial Meningiomas: A Distinct Subtype Of Nf2-Mutant Tumors

Jacob Francis Baranoski
Yale School of Medicine

SMARCB1-Mutant Intracranial Meningiomas:

A distinct subtype of *NF2*-mutant tumors

A Thesis Submitted to
the Yale School of Medicine
in Partial Fulfillment of the Requirements for the
Degree of Doctor of Medicine

by
Jacob F. Baranoski
2015

ABSTRACT

SMARCB1-MUTANT INTRACRANIAL MENINGIOMAS: A DISTINCT SUBTYPE OF *NF2*-MUTANT TUMORS.

Jacob F. Baranoski, Victoria E. Clark, Akdes Serin, and Murat Gunel.

Department of Neurosurgery, Yale, School of Medicine, New Haven, CT.

Meningiomas are the most common central nervous system primary tumors. Mutations in the tumor suppressor gene *Neurofibromin 2* (*NF2*), located on chromosome 22 (Chr22), are present in 40-50% of sporadic meningiomas. In a subset of non-*NF2*-mutant meningiomas, recent studies have identified tumorigenesis driver mutations in the genes *TRAF7*, *AKT1*, *KLF4*, and *SMO*. However, the genetic basis for the marked clinical and histological heterogeneity that exists among *NF2*-mutant/Chr22-loss meningiomas remains to be established. In this study, we utilized next-generation sequencing techniques to identify and screen a large cohort of *NF2*-mutant/Chr22-loss meningiomas for concurrent co-driver mutations in novel genes that may contribute to the observed clinical and histological heterogeneity of these tumors.

We identified 25 *NF2*-mutant/Chr22-loss meningiomas that harbored concurrent somatic mutations in the *SMARCB1* gene. *SMARCB1* codes for a component of the SWI/SNF complex and is involved in epigenetic modification via nucleosome modulation and chromatin remodeling. SMARCB1 is also known to interact with

GLI1, an important effector of the Hedgehog pathway, and EZH2, a member of the Polycomb-group proteins that is capable of epigenetically silencing gene expression via histone methylation. *SMARCB1* somatic mutations have previously been associated with the highly aggressive malignant rhabdoid tumors and germline variants have previously been identified as the driver mutation responsible for familial schwannomatosis. Notably, a subset of patients with familial schwannomatosis develop multiple meningiomas as part of their disease course. We performed RNA expression analysis to determine gene expression differences in *SMARCB1*-mutant meningiomas versus non-*SMARCB1*-mutant meningiomas. Unsupervised hierarchical clustering demonstrated that the expression profiles of *SMARCB1*-mutant meningiomas cluster similarly to other *NF2*-mutant/Chr22 loss meningiomas. However, within this superfamily, *SMARCB1*-mutant meningiomas form distinct subgroups. This differential clustering is due, at least in part, to increased *GLI1* and *EZH2* expression suggesting that *SMARCB1*-mutant tumors represent a distinct genetic subtype of *NF2*-mutant meningiomas.

Genomic-clinical correlates for *SMARCB1*-mutant tumors showed no significant differences in this cohort in age at time of surgery (median = 64 years), gender predilection (80% female), or low-grade histologic subtype when compared to the natural history literature. However, the *SMARCB1*-mutant meningiomas were predominantly midline tumors (71%) with increased propensity to being high-grade lesions (36%), despite remarkable chromosomal stability. These clinical findings strongly paralleled our genetic data suggesting that increased expression of

GLI and *EZH2* may, respectively, contribute to the midline tumor location and serve as a substitute for widespread chromosomal instability in high-grade lesions. These results demonstrate that *SMARCB1*-mutant meningiomas represent a genetically and phenotypically distinct sub-group of *NF2*-mutant meningiomas and partially contribute to the observed clinical heterogeneity of convexity lesions. This study also suggests potential targets for therapeutic interventions that warrant future investigation.

ACKNOWLEDGMENTS

I attribute my accomplishments to the generous contributions of many helpful individuals. I would first and foremost like to thank Dr. Murat Gunel. As my clinical attending, academic advisor, and PI, he has seen both the best and worst of my capabilities. He is an exceptional teacher and mentor and I am extremely fortunate to have been afforded the opportunity to learn from and work with him. I owe my success to his support and guidance. He has helped me become a better student, future physician-scientist, and more importantly, a better person.

I thank all the members of the Gunel Laboratory. You have all been essential to both the completion of this project and in making the process enjoyable and exciting.

I am especially grateful to Victoria Clark who has been my greatest ally, resource, and friend through this process. Without her support and guidance, none of this would have been possible.

I acknowledge Dr. Akdes Serin, Dr. Kaya Bilgüvar, Dr. Zeynep Erson-Omay, Dr. Jie Li, Geneive Carrión-Grant, Dr. Ahmet Okay Caglayan, Dr. Alexander Vortmeyer, Mark Youngblood, Dr. Octavian Henegariu, Dr. Ketu Mishra-Gorur, and Dr. Katsuhito Yasuno for their insight and invaluable contributions to this research.

I thank my thesis committee, Dr. Nenad Sestan and Dr. Joseph Piepmeier, and my thesis department chair, Dr. Angeliki Louvi, for their support and guidance.

I acknowledge the leadership and members of The Yale Center for Genome Analysis and the Yale Keck DNA Sequencing Facility for their assistance.

I thank the Yale School of Medicine Dean's Office and the Office of Student Research for their help and support.

This project was funded by an NIH – CTSA TL1 fellowship training grant.

On a personal note, I would like to thank all of the great friends that I have met over these five years. You have all given essential value to my time here and your friendships mean more than I think any of you realize.

Finally, I would like to thank my parents and brother, Stephen. It is their support and hard work that has gotten me to where I am today – I literally could not have done any of this without them. I owe them a debt of gratitude that I will never be able to fully repay.

Thank you.

TABLE OF CONTENTS

INTRODUCTION

Meningiomas – Clinical and Histological Overview

Meningiomas are central nervous system (CNS) tumors that arise from the meninges. They are the most common primary CNS tumor (35%) with a prevalence of approximately 170,000 cases and approximately 22,000 new cases diagnosed annually in the United States(1). The World Health Organization (WHO) classifies meningiomas as grade I to grade III based on morphologic and histopathological criteria(2). Histologic WHO grade I lesions are benign and are by far the most common. However, while previous studies estimated that >90% of meningiomas were grade I (3, 4), contemporary reports and retrospective analysis of previous studies now estimate that grade I lesions more likely comprise approximately 80% (5-7). Grade I lesions can be further classified by histologic characteristics into the following subtypes: meningothelial, fibrous, transitional, psammomatous, angiomatous, microcystic, secretory, lymphoplasmacyte-rich, or metaplastic meningioma (5, 8). Grade I lesions are generally amenable to surgical resection. However, even with complete surgical resection, these lesions have a relatively high rate of recurrence (10-18%) at 5 years after surgery (9, 10). Grade II meningiomas ("atypical") are thought to comprise 5-20% of all meningiomas (3, 5-8, 11). These lesions are histologically characterized by an increased mitotic index ($\geq$ 4 per 10 high-powered fields) and the presence of foci of necrosis (2, 8). Clear-cell and choroid variants are also characterized as Grade II lesions (5, 8). Grade III lesions

("anaplastic"), comprising only 1-5% of all meningiomas (3, 5, 6), are characterized by a significantly greater mitotic index ($\geq$ 20 per 10 high-powered fields) and multiple, large foci of necrosis (5, 8). Rhabdoid and papillary meningiomas are also considered grade III (5).

Like grade I meningiomas, grade II and grade III lesions can be amenable to surgical resection; however, these higher-grade tumors have even higher rates of recurrence and carry significantly more grave prognoses. Grade II meningiomas have a reported 40% recurrence rate at 5 years following total resection and a 5 and 10-year overall survival rate of 78-95% and 53-79%, respectively, even with optimal surgical treatment (5, 11-13). Grade III lesions have a recurrence rate approaching 80% at 5 years following total resection and with a 5 and 10-year overall survival rate of only 44-64% and 14-34%, respectively, following treatment. One factor contributing to the poor prognosis carried by the high-grade meningiomas is the lack of effective chemotherapeutic therapies to supplement surgical and radiation interventions (14). It is believed that the majority of these higher-grade tumors arise *de novo*; however, there are a number of case reports that describe the progression of grade I lesions to both atypical and anaplastic variants (15, 16).

In addition to the WHO grading system, meningiomas can also be classified by their location within the CNS. The majority (90-98%) are found intracranially, with only 2-10% occurring in the spine (4, 8). Within the cranium, meningiomas can be described as either "skull base" or "convexity" lesions. Skull base lesions arise from

the meninges that overlie the boney surfaces of the sphenoid wing, olfactory groove, suprasellar region, or posterior cranial fossa. Convexity meningiomas (including falcine and parasagittal lesions) are tumors that grow from the meninges over the cerebral hemispheres.

Classified by location, convexity meningiomas are the most common (approximately 25-40%) (17, 18). Given their locations on the surface of the brain, convexity lesions are generally more amenable to surgical resection compared to skull base tumors. However, multiple studies have identified convexity meningiomas as having significantly increased propensities to recur and to present as *de novo* grade II or grade III lesions (18-22). In other words, the tumors that have the easier surgical approach are the ones with an increased likelihood of being malignant. Furthermore, there is marked heterogeneity among convexity meningiomas in terms of location, histological type, grade, and propensity to recur.

The primary treatment for both benign and higher-grade meningiomas remains surgical resection. Radiation therapy has been frequently used as an adjuvant to surgical resection; however, its use remains controversial (9, 10, 12, 23). Further, the use of standard chemotherapeutic medications as a therapy has been largely ineffective (14).

Cancer Genetics

With the recent developments in next-generation sequencing technologies, the field of cancer and clinical genetics has experienced a period of exponential growth (24-26). These technologies now allow for a rapid, unbiased, and comprehensive analysis of the genetic mutations underlying tumorigenesis (27) and inheritable disorders (28-31). Research utilizing these techniques has advanced our understanding of the pathogenesis of numerous cancers including leukemias and lymphomas (32-42), melanoma (43, 44), renal cell carcinoma (45, 46), head and neck squamous cell carcinoma (47-49), breast carcinomas (50-53), hepatocellular carcinoma (54, 55), lung (56, 57), esophageal (58-61), pancreatic (62), prostate (63), gynecologic cancers (64-66), and others.

CNS tumors have also been studied using these methods, leading to the identification of genetic mutations associated with ependymomas (67), medulloblastomas (68), craniopharyngiomas (69), solitary-fibrous tumors (70), and gliomas (71, 72).

The identification of the genetic aberrations associated with tumor development not only helps define the pathophysiology and molecular mechanisms driving tumorigenesis, but also identifies potential therapeutic targets for chemotherapeutic and immunotherapeutic regimens (73).

Broadly, the genetic aberrations associated with various cancers can be classified as either “germline” or “somatic”. Germline mutations are detectable and heritable variations in the germ cell lineage and are transmitted to offspring following the usual patterns and rules of inheritance. A germline mutation results in a constitutional mutation in the offspring - that is, the mutation is present in every cell. The role that the inherited genetic aberration plays in the development of cancer depends on the characteristics and downstream effects of the mutation, as well the expression and inherent role of the mutated gene and the pathophysiology of the disease state. For example, Li-Fraumeni syndrome is caused by a germline loss of the *p53* gene which results in the development of a variety of cancers (74). The effect of the inherited mutation may also be a very specific, stereotyped tumorigenesis – as in familial adenomatous polyposis syndrome, caused by a germline mutation in the *APC* gene (75).

In contrast to germline mutations, somatic (also termed “acquired”) mutations are not heritable and are only present in cells that originate from the primarily affected cell. These mutations may initially affect only one copy of the gene and can arise from DNA damage or errors during DNA replication. A well-characterized somatic mutation associated with cancer is the *BRAF* V600E variant that was found to drive the tumorigenesis of melanomas (76).

An example helps to clarify the distinction between germline and somatic mutations as they pertain to tumor development. In a patient with lung adenocarcinoma, a

sample of the tumor is genetically analyzed and is found to harbor a mutation in gene X. If this mutation is a germline mutation, then 1.) the patient will have inherited this mutation from his parents; 2.) this exact mutation will be present in the DNA of all the patient's cells, including non-tumor cells (white blood cells, for example); and 3.) the patient may pass this mutation on to offspring. In contrast, if the mutation in gene X is a somatic mutation, then 1.) the mutation will not have been inherited but rather will have arisen within a cell within the patient's lungs, either *de novo* or in response to some environmental factor – perhaps as a result of exposure to cigarette smoke 2.) this mutation will not be present in the DNA of other, non-tumor cells within in the patient (white blood cells, for example); and 3.) the patient will not pass this mutation on to offspring.

Genetics of Meningiomas

Investigations of the genetics of meningiomas have focused on both heritable, syndromic cases and sporadic lesions. The results of these studies have identified a number of genetic mutations associated with CNS meningiomas and have demonstrated that both germline and somatic aberrations can play a role in meningioma tumorigenesis.

Germline Mutations Associated with Meningiomas

The most notable inherited syndrome associated with meningiomas is Neurofibromatosis type 2, an autosomal dominant disorder characterized by the development of multiple neoplastic lesions. Neurofibromatosis type 2 results from a mutation in the tumor suppressor gene *Neurofibromin 2* (*NF2, merlin*), which is located on the long arm of chromosome 22 (Chr22) (Chr22q12.2) (12, 77). *NF2* encodes the tumor suppressor protein Merlin, which localizes to the cell membrane and has been implicated in regulating cell growth and motility (12, 78-80). In addition to the pathognomonic bilateral acoustic neuromas (81-83), approximately 50% of patients develop meningiomas (84, 85). Interestingly, many patients with Neurofibromatosis type 2 associated meningiomas will have multiple lesions (meningiomatosis) (84, 86). Patients with Neurofibromatosis type 2 also tend to develop meningiomas that both occur at an earlier age and are more frequently high-grade compared to patients who develop non-syndromic, sporadic tumors (86-88). These findings established a role for *NF2* mutations in the development of meningiomas; however, a specific mechanism of *NF2* mutations in the development and progression of higher-grade lesions has not been elucidated (5, 12).

Aside from the *NF2* mutation, there is only a short list of other germline mutations that have been associated with heritable meningiomatosis. These studies comprise only a handful of case reports and series that describe a small number of families. Of these, the most consistently reported mutated gene is *SMARCB1* - SWI/SNF related,

matrix associated, actin dependent regulator of chromatin, subfamily b, member 1. *SMARCB1* (discussed in detail below) is located on the long arm of Chr22 (22q11.23) and is thought to act as a tumor suppressor. Germline mutations in *SMARCB1* have been associated with the development of malignant rhabdoid tumors of the kidney, atypical teratoid/rhabdoid tumors (AT/RT) of the CNS, and extra-renal rhabdoid tumors (89-92).

Germline *SMARCB1* mutations have also been shown to play a role in familial schwannomatosis – a form of neurofibromatosis characterized by multiple schwannomas, but without bilateral vestibular schwannomas (93-95). Approximately 50% of patients with familial schwannomatosis harbor a germline loss-of-function mutation in *SMARCB1* (96). A subset of patients with *SMARCB1*-associated schwannomatosis also develop multiple meningiomas (97-99). Interestingly, one study reported that intracranial meningiomas associated with germline *SMARCB1* mutations have a predilection to form along the falx cerebri – a midline meningeal fold that separates the cerebral hemispheres (99).

Somatic Mutations Associated with Meningiomas

Somatic genetic mutations play a role in the development of meningiomas that arise sporadically – i.e. without a familial predisposition. Compared with germline mutations, sporadic mutations give rise to more variable and non-syndromic

disorders that challenge specific characterization. There are, however, similarities in the gene mutations associated with sporadic meningiomas. Not surprisingly, just as germline *NF2* mutations are associated with syndrome meningioma formation, approximately 40-50% of all sporadic meningiomas have somatic mutations in the tumor suppressor gene *NF2* and/or loss of chromosome 22 (Chr22)(5, 8, 12, 100-103). As described above, *NF2* is located on the long arm of Chr22 (Chr22q12.2) (12, 77).

Mutations in *NF2* / Chr22-loss may initiate meningioma tumorigenesis, but may not necessarily drive tumor progression to higher-grade lesions (5, 12). However, other large-scale chromosomal abnormalities may be involved in tumor progression. Some chromosomal abnormalities have been associated with higher-grade lesions include loss of Chr1p, 6q, 9p, 10q, 14q, 18q and gain of Chr1q 9q, 12q, 15q, 17q, 20q (104-107). However, the precise genes responsible for either the progression of grade I meningiomas to higher-grade lesions or the *de novo* formation of atypical and anaplastic meningiomas have not been identified (5, 12). Further, while mutations in *NF2* and/or loss of Chr22 have been identified in a large percentage of meningiomas, approximately 50-60% of sporadic meningiomas do not harbor these genetic aberrations.

Recent studies have begun to examine the genetic mutations responsible for the formation of non-*NF2* / non-Chr22-loss sporadic meningiomas. In 2013, a study by Clark et al. identified mutations in *TRAF7*, *AKT1*, *KLF4*, or *SMO* in 60% of *non-NF2*

meningiomas (101). Additional studies have confirmed the presence of *AKT1* or *SMO* mutations in non-*NF2* meningiomas (108) and mutations in *TRAF7* and *KLF4* in secretory meningiomas (109). Clark et al. found *TRAF7* mutations in approximately 25% of all meningiomas (101). *TRAF7* codes for an E3 ubiquitin ligase and plays a role in the degradation of anti-apoptotic molecules (110); thus mutations in *TRAF7* may have a net anti-apoptotic effect.

A subset of meningiomas with *TRAF7* mutations was also found to have concurrent mutations in either *KLF4* or *AKT1* (3). *KLF4* codes for a transcription factor that plays a critical role in the regulation of cellular differentiation; it is most prominently known for being one of the four transcription factors capable inducing the transformation of human somatic cells into pluripotent stem cells (111). Mutations in *AKT1* have been previously shown to induce constitutive activation of the PI3K/AKT pathway and promote cell growth, proliferation, and survival (112). *SMO* encodes Smoothened, a receptor in the Hedgehog signaling pathway (113). Mutations in *SMO* have been previously associated with tumor formation and development of basal cell carcinoma (114).

Somatic *SMARCB1* mutations have also been associated with in 8 sporadic meningiomas (101, 108, 115, 116); however, the precise genomic architecture and phenotypic effects of these mutations have not been well described. In 2001, Schmitz et al. was the first to report a somatic mutation in *SMARCB1* in sporadic meningiomas (116). The investigators identified four meningiomas with a recurrent

somatic mutation in *SMARCB1*. These tumors all also possessed a predicted loss-of-function mutation in *NF2* and/or loss of a copy of Chr22. In 2003, Rieske et al. reported finding one meningioma (out of eighty screened via targeted Sanger screening) that possessed a heterozygous, predictive loss-of-function mutations in *SMARCB1* (115). However, no further genomic analysis (including *NF2* status or demonstration that the identified mutation was indeed somatic) or clinical correlations were provided. Clark et al. did identify 2 sporadic meningiomas that harbored a somatic *SMARCB1* mutation (101). Both of these tumors also possessed a concurrent loss-of-function mutation in *NF2.* Likewise, Brastianos et al. also reported a single sporadic meningioma that possessed a somatic *SMARCB1* mutation with a concurrent mutation in *NF2* (108). Again, however, none of these studies provided any additional, in-depth analysis of the genomic architecture of these lesions or evidence of any effect on clinical presentation or tumor phenotype conferred by the mutation in *SMARCB1*.

Interestingly, in addition to discovering mutations in genes previously not known to be associated with meningioma development, Clark et al. also described a pattern of the genetic profiles for skull base meningiomas. That is, they found that specific gene mutations correlated with the locations of meningiomas of the anterior skull base. Specifically, they found that tumors originating from the skull base in the posterior cranial fossa were most likely to harbor mutations in *NF2* while anterior skull base tumors tended to possess mutations in *TRAF7*; tumors located in the sphenoid wing predominantly harbored *KLF4* mutations; meningiomas with *AKT1*

or *SMO* mutations were located along the midline of the anterior skull base (101). A summary of these results is shown in Figure 1., adapted from Clark et al., 2013 (101).

Figure 1.

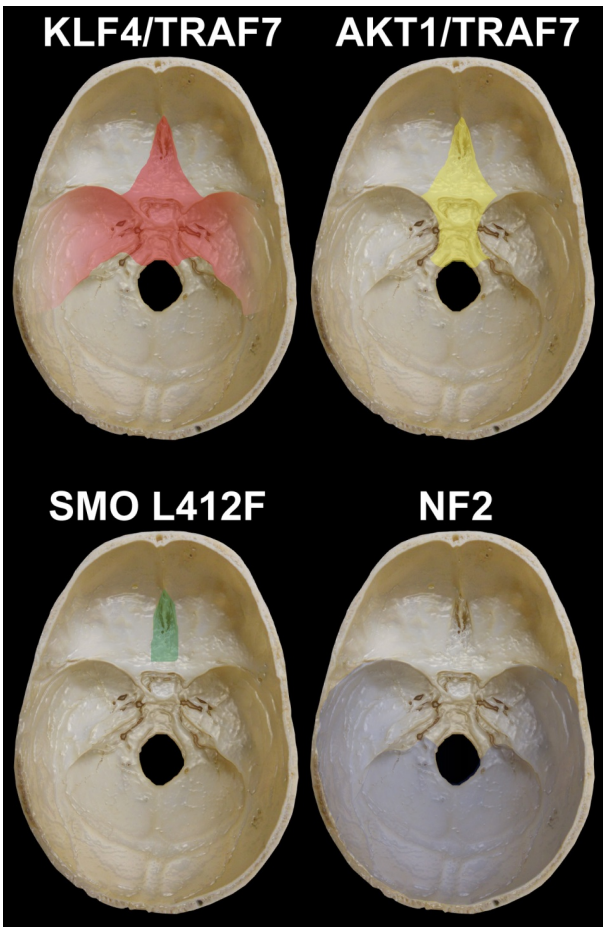

Figure 1. "Mutation Map" for Skull Base Meningiomas

Meningiomas arising along the skull base tend to possess a specific, stereotyped mutation driving tumor formation based on tumor location. Specifically, meningiomas arising from anterior skull base tended not to posses the *NF2* / Chr22-loss mutations. Instead, tumors arising from the sphenoid wing tended to harbor *KLF4* / *TRAF7* mutations, midline tumors possessed *AKT1* / *TRAF7* mutations, and tumors originating from the olfactory groove tended to harbor *SMO* mutations. In contrast, meningiomas arising from the posterior skull base tended to be *NF2* / Chr22-loss.

Figure adapted from Clark et al., 2013. (101)

A critical next step in the genetic study of meningiomas is the investigation of the correlation between tumor characteristics and gene mutations in sporadic meningiomas. Extending the correlation between location and genetic mutation (shown by Clark et al.), we hypothesized that a "mutation map" for convexity meningiomas will also help describe the association between specific gene mutations and meningioma location.

Clark et al. were also able to correlate the mutational profiles of meningiomas with certain histologic characteristics of skull base lesions. In their investigation, skull base lesions tended to be grade I lesions while convexity tumors had a higher percentage of grade II and grade III lesions (101); this is consistent with the findings of previous epidemiologic studies (18-22, 101). Further, they identified that secretory meningiomas were more likely to harbor concurrent mutations in both *TRAF7* and *KLF4* (101). Again, similar to the "mutation map", we hypothesized that correlations between the mutational profile and tumor phenotype for convexity meningiomas may exist and can be identified via next-generation high-throughput genetic screening and whole-exome sequencing techniques.

A number of other studies have attempted to identify the specific genes responsible for the observed clinical and histological differences among *NF2*/Chr22-loss convexity meningiomas, the development and progression of higher-grade tumors, and tumorigenesis of non-*NF2* convexity lesions. However, what is needed is an unbiased genomic approach to investigate subsets of meningiomas. Genomic

characterization of these lesions, including whole-exome sequencing to identify unique and/or concurrent driver mutations and epigenetic and expression analyses have the potential to identify factors that: 1.) account for the clinical and histological variability among *NF2-loss* convexity meningiomas; 2.) drive formation of *non-NF2* convexity meningiomas; 3.) are responsible for tumor progression to and/or *de novo* formation of higher-grade lesions; 4.) predispose tumors to recur; 5.) and, eventually, help to inform treatment and clinical management.

SMARCB1

Component of the SWI/SNF Complex

SMARCB1 (also known as *SNF5, INI1,* or *BAF47*) codes for a component of the SWI/SNF complex. This gene is located on the long arm of Chr22 (22q11.23), 6 megabases away from the *NF2* locus; the gene contains nine exons and spans approximately 50 kilobases (92). *SMARCB1* codes for a protein that is comprised of three highly conserved regions – two repeat domains (Rpt1 and Rpt2) and a C-terminal putative coiled coil domain (117). The precise role of these domains have not been fully described. The SMARCB1 protein is a known core component of the SWI/SNF or BAF chromatin-remodeling complex (118).

The SWI/SNF complex regulates gene expression via ATP-dependent nucleosome modulation and subsequent chromatin remodeling (119-121). Chromatin is the network of DNA and histone proteins that packages DNA into chromosomes (122). A nucleosome is a subunit of chromatin consisting of DNA wrapped around eight histone cores. The structure of chromatin can be remodeled to alter how tightly DNA is packaged. This remodeling is one method by which the cell regulates gene activity – DNA that is tightly packed is less transcribed, and thus gene expression is lower, compared to DNA that is loosely packaged, and thus more highly expressed (121).

The SWI/SNF complex remodels chromatin via mobilizing nucleosomes and catalyzing the ejection and insertion of histone octamers (123). The complex has also been demonstrated to play a role in transcription factor binding, further highlighting the capacity of SWI/SNF to regulate gene expression (123, 124). The protein coded for by SMARCB1 is a core SWI/SNF complex subunit that is present in all known variants of the SWI/SNF complex; the genetic sequence of *SMARCB1* is very highly conserved (118). The SMARCB1 subunit has been implicated to play a role in the recruitment of the SWI/SNF complex to specific target genes (125, 126).

Via its broad role in the regulation of DNA transcription, the SWI/SNF complex has been demonstrated to play a role in numerous processes including DNA repair (127-129), cell cycle progression (130-133), cell proliferation and differentiation (134-138). Importantly, there is emerging evidence that SWI/SNF complex also acts a

tumor suppressor (139). Mutations to integral components of the complex have been associated with the development of numerous tumors including various forms of renal (140), pancreatic (141, 142), hepatocellular (143), breast (144-147), ovarian (148, 149), and lung (150-153) cancers and medulloblastomas (154).

Role in Tumorigenesis

Aberrations in the SMARCB1 subunit of the SWI/SNF complex have been associated with tumorigenesis. In addition to the association of germline and somatic *SMARCB1* mutations with schwannomas and meningioma formation discussed above, loss-of-function mutations in *SMARCB1* have been identified in malignant rhabdoid tumors (89, 90, 92, 155), chondrosarcomas, atypical teratoid/rhabdoid tumors (AT/RT) of the CNS (156), epitheliod sarcomas (157), and chordomas (158). These mutations occur both as somatic mutations in sporadic cases and as germline mutations in familial cases, as in a condition termed rhabdoid predisposition syndrome (90, 156). The role of *SMARCB1* as a tumor suppressor has further been demonstrated in animal studies. Prior research has found that mice that are heterozygous for the *SMARCB1* allele develop rhabdoid-like tumors of the CNS and soft tissues of the first branchial arch (159-162).

The clinical and animal model results nicely parallel some of the findings from studies examining the molecular mechanisms and pathophysiology of *SMARCB1*

mutations. Using microarray analysis, one study found that the mRNA expression of p16INK4A, a tumor suppressor molecule coded for by the gene *CDKN2A,* is decreased as a result of *SMARCB1* inactivation (163). Loss of function mutations in *CDKN2A* have previously been well described in a wide variety of cancer types (164). A follow-up study demonstrated that it is indeed loss of p16INK4A activity that is required for *SMARCB1* mediated tumorigenesis in malignant rhabdoid tumor cells *in vitro* (125). Additional studies have found that cyclin D1 expression, a protein that promotes cell cycle progression, is increased in *SMARCB1*-null malignant rhabdoid tumor cells and, further, that re-expression of SMARCB1 in a rhabdoid tumor cell line resulted in SMARCB1 binding to the cyclin D1 gene (CCND1) promoter leading to decreased cyclin D1 expression and cellular quiescence (121, 165, 166). Interestingly, pharmacological inhibition of cyclin D1 has been shown to limit the growth of malignant rhabdoid tumor cells. These findings suggest that cyclin D1 inhibitors may serve as a potential therapeutic regimen in patients with SMARCB1-deficient malignant rhabdoid tumors and potentially other *SMARCB1*-mutated tumors (167-169).

The SWI/SNF complex, and SMARCB1 specifically, are also known to interact with c-Myc – a transcription factor and well characterized oncogene that is frequently overexpressed in cancer (170, 171). Previous work has demonstrated that the SWI/SNF complex is capable of directly repressing c-Myc expression (172). Interestingly, c-Myc expression has been shown to be increased in *SMARCB1*-null rhabdoid tumor cells, suggesting that c-Myc and its downstream targets may play a

role in *SMARCB1*-mutant rhabdoid tumor as well as other SWI/SNF-aberrant cancers (121, 165, 173).

Recent work has implicated the Hedgehog Pathway in *SMARCB1*-mutant tumors. The Hedgehog pathway is involved in embryogenesis and has well described roles in limb development and the patterning of the midline structures (174, 175). Loss of Sonic Hedgehog, a key ligand of the Hedgehog pathway, results in holoprosencephaly (176) – an embryologic disorder in which the forebrain does not develop into two hemispheres. The defects range from severe which results in fetal demise through milder forms where brain development is normal but face and eyes are affected. Recent studies have identified aberrant activation of the Hedgehog pathway to play a role in a number of cancer types. This aberrant activation typically is the result of mutation in one or more of the upstream components of the pathway (177). Mutations to the Hedgehog pathway have now been associated with both syndromic and sporadic basal cell carcinomas (*PTCH1* (178, 179) and *SMO* (180, 181)), medulloblastomas (*PTCH1* and *SUFU* (182)), and even meningiomas (*SMO* (101, 108)).

GLI1 is an important transcription factor of the Hedgehog pathway and plays key roles during embryogenesis. Recently, the SMARCB1 component of the SWI/SNF complex was found to interact with GLI1. This study demonstrated that inactivation of SMARCB1 resulted in aberrant upregulation of the Hedgehog pathway and increased GLI1 mRNA expression (183). This SMARCB1-null-mediated aberrant

increase in Hedgehog pathway signaling was necessary for the growth of rhabdoid tumor cells (183). These results are consistent with studies demonstrating increased GLI1 expression in basal cell carcinomas resulting from mutations upstream in the Hedgehog pathway (184, 185). Taken together, these works highlight a potential role for the deregulation of the Hedgehog pathway by SWI/SNF component aberrations (specifically SMARCB1) in tumorigenesis.

SMARCB1 mutations may also play a role in tumorigenesis via epigenetic alterations. Epigenetic alterations refer to somatically heritable changes in gene expression that are the result of chromatin modification rather than genetic mutation (186). SMARCB1 and the SWI/SNF complex are capable of chromatin remodeling via ATP-dependent nucleosome modulation (119-121). While numerous genetic mutations and wide-spread genomic instability are largely considered the hallmark of tumor cells, recurrent epigenetic alterations have been also been hypothesized to play a key role in tumorigenesis and tumor progression (187). This hypothesis suggests that epigenetic changes that result from aberrations in the regulation of chromatin remodeling can augment and/or be a substitute for widespread genomic instability in the genesis of aggressive cancers and high-grade tumors. Intriguingly, research examining the role of *SMARCB1* mutations in the highly aggressive malignant rhabdoid tumors supports this hypothesis. A 2008 study found that SMARCB1 inactivation had no effect on the DNA damage response and, further, the majority of *SMARCB1*-mutant tumors are remarkably stable, harboring relatively few genetic point mutations and chromosomal alterations (such as large scale amplifications or

deletions) compared to what one would expect for such an aggressive tumor type (165).

An additional mechanism by which *SMARCB1* mutations may contribute to tumorigenesis is via an antagonistic interaction that exists between the SWI/SNF complex and Polycomb-group (PcG) proteins. PcG proteins are capable of epigenetically silencing the expression of a gene via histone methylation, resulting in chromatin remodeling (188-190). Studies have demonstrated that the SWI/SNF complex and PcG proteins have an antagonistic relationship, such that the SWI/SNF complex is required for specific gene activation and the PcG proteins are required for specific gene repression (191-194). Alterations in PcG proteins (especially the PcG protein EZH2) are associated with various cancers. Interestingly, EZH2 expression levels – that have been found to be elevated in numerous cancers and are often correlated with advanced disease stages and poor clinical prognosis (195) – are elevated in *SMARCB1*-mutant tumors (194). Further, recent work has demonstrated that re-expression of SMARCB1 in a *SMARCB1*-null cell line results in PcG expulsion from the *CDKN2A* locus, rescuing the expression and function of this critical tumor suppressor molecule (191). In addition to the *CDKN2A* locus, rhabdoid tumor cells lacking *SMARCB1* display widespread suppression of other PcG protein target genes (191, 194). Collectively, these findings demonstrate that an aberration in the antagonistic relationship between EZH2 and SMARCB1 may be the driving mechanism by which these *SMARCB1*-mutant tumors form and/or contribute to their aggressive nature. These results also suggest that pharmacologic inhibition of

EZH2 may serve as a potential therapeutic target for patients with *SMARCB1*-mutant tumors.

STATEMENT OF PURPOSE AND SPECIFIC AIMS

Specific Aim I: Genetically characterize NF2-loss meningiomas and identify additional novel and/or concurrent activating or loss-of-function driver mutations that contribute to heterogeneity of NF2-loss tumors.

Mutations in the tumor suppressor gene *Neurofibromin 2* (*NF2, merlin*; located on chromosome 22) are present in 40-50% of sporadic meningiomas. Recently, studies have begun to examine the genetic mutations responsible for the remaining 50-60% of meningiomas that do not possess mutations in or the loss of *NF2.* However, despite these recent discoveries, no study has effectively established the genetic basis for the marked clinical and histological heterogeneity that exists among *NF2*-mutant/Chr22-loss convexity meningiomas.

Specific Aim II: Perform epigenetic and expression analyses to further genomically characterize NF2/Chr22-loss convexity meningiomas.

Alterations to in gene expression can further account for the discrepancies in tumor biology and clinical behavior as well as suggest a mechanism for the observed heterogeneity among convexity meningiomas. Importantly, characterization of these aberrant pathways and mechanisms is a critical step in identifying potential targets

for chemotherapeutic interventions that may one day serve as adjunctive therapy for recurrent and high-grade lesions.

Specific Aim III: Compare and correlate clinical, radiologic, and histological features of convexity and spinal meningiomas with their genetic architecture.

Clark et al. described a distribution of genetic mutation profiles for skull base meningiomas such that meningiomas located in specific regions of the skull base were most likely to possess mutations in a specific gene or genes. We believed that a similar "mutation map" – a mutation gradient or distribution – may exist for convexity and spinal meningiomas. Further, we sought to correlate specific clinical, radiologic, and histological characteristics of meningiomas with their genetic architecture.

RESEARCH DESIGN AND METHODS

Collection of Meningioma Samples and Clinical Data

Institutional Review Board, including the Yale Human Investigation Committee, approvals for genetic studies and written consent from all study participants were obtained at the participating institutions. (HIC Protocol # 9406007680). Demographic information along with formal pathology reports, pre-operative magnetic resonance imaging (MRI) studies, and pre-operative radiology reports were collected from study subjects. Meningiomas of varying grades, histological classifications, and locations were included. Patients were included regardless of age or gender. Patients with tumors treated with radiation therapy prior to resection and patients who exhibited any obvious clinical manifestations of syndromic disease (Neurofibromatosis, etc.) were excluded from analysis

Resected meningiomas were histologically characterized and graded by a board-certified pathologist according to WHO guidelines. This was performed either by members of the Department of Pathology at the Yale School of Medicine or the collaborating institution. A sample of tissue was then frozen and sent to Dr. Gunel's laboratory, along with a sample of blood from that patient (if available), for processing.

Radiographic information, including tumor location, was provided by radiology reports and characterization by board-certified radiologists and/or neurosurgeons at participating institutions.

Correlation between clinical information and genetic analyses were performed to identify potential genetic and phenotypic relationships. All clinical correlations and analyses reported in this study were performed by Jacob Baranoski.

Nucleic Acid Isolation

Genomic DNA and RNA were extracted from tumor tissues using QIAgen Allprep DNA/RNA/protein Mini Kit (Qiagen Science, MD) according to the manufacture's standard protocols. DNA from patient blood samples was extracted using QIAgen DNeasy Blood & Tissue Kit (Qiagen Science, MD) according to the manufacture's standard protocols.

DNA extracted from tumor and blood samples underwent quality control metrics, including quantification (via Nanodrop and/or PicoGreen analyses using standard protocols), DNA re-purification using QIAgen kits according to the manufacture's standard protocols, and allocation for one or more of the sequencing methods detailed below. These protocols were performed by Jacob Baranoski.

Genomic Analyses

Whole-Exome Sequencing and Analysis

Human solution-capture exome arrays from Nimblegen/Roche (Roche Nimblegen, Inc.) were used to capture the exomes of blood and tumor samples according to the manufacturer's protocol with modifications, as described previously by Bilguvar et al., 2010 (26). Briefly, genomic DNA was captured on a NimbleGen 2.1M human exome array according to the manufacturer's protocols (Roche Nimblegen, Inc.) with slight modifications at the Yale Center for Genome Analysis (YCGA) at Yale University. Genomic DNA was sheared via sonication and the resulting sheared fragments were ligated to adaptors. These ligated fragments were fractionated via agarose gel electrophoresis and the desired size fragments were excised. Excised DNA was then amplified via PCR, purified, and hybridized to the capture array using the manufacturer's buffer and protocol (Roche Nimblegen, Inc.). The array was washed according to manufacture's protocol, with modifications, and using the manufacturer's buffers (Roche Nimblegen, Inc.). Bound genomic DNA was eluted using 125 mM NaOH for 10 min at room temperature, purified, and then amplified via PCR. The captured DNA libraries were then sequenced on Illumina HiSeq instruments using 74 base pairs paired-end reads by multiplexing two tumor samples or six blood samples per lane. Detailed descriptions of these methods are provided by Bilguvar et al. (26) and Choi et al. (196). Samples were submitted by

Jacob Baranoski and Victoria Clark. Exome capture and sequencing protocols were performed by YCGA.

Exome sequence analysis was performed using a bioinformatics pipeline developed by the Gunel Laboratory utilizing in-house written scripts as well as commercially and publicly available software, as described previously by Clark et al., 2013 (101). Briefly, sequence reads that passed the Illumina quality filter were selected for analysis using an in-house written bioinformatics pipeline. First, low-quality reads were further filtered out using the FASTX-Toolkit software (http://hannonlab.cshl.edu/fastx_toolkit/) and PCR primer-contaminated sequence segments were trimmed using cutadapt software, version 0.9.5 (http://code.google.com/p/cutadapt/). Selected reads were then aligned to the human genome reference sequence (version GRCh37) using Stampy (version 1.0.16) (197) and BWA (version 0.5.9-r16) (198) software. PCR duplicates were identified using the MarkDuplicates algorithm from Picard (version 1.47, http://picard.sourceforge.net/) and discarded. Sequence quality metrics, including the fraction of unique read pairs, the fraction of aligned reads, and depth of coverage, were collected for each sample via the CollectAlignmentSummaryMetrics and CalculateHsMetrics algorithms of the Picard software. Multi-sequence local realignment around known sites was performed along with base quality score recalibration using the Genome Analysis Toolkit (GATK, version 1.5-20) (199). Point mutations, small insertions/mutations were identified using the UnifiedGenotyper algorithm from the GATK software package (199). Called variants were filtered

using quality metrics for allelic and sample depth of coverage, mapping quality, ratio of reference and non-reference allele reads, consistency between number of allelic reads and haplotype scores, and coverage-adjusted variant read quality. Finally, variant alleles were annotated using the Ensembl database (version 66) with the help of Variant Effect Predictor (version 2.4) software (http://useast.ensembl.org/info/docs/variation/vep/vep_script.html). A detailed description of these methods is provided by Clark et al. (101). Sequence files were run through this pipeline by Victoria Clark. Sequence results were analyzed by Jacob Baranoski and Victoria Clark.

Custom Amplicon Sequencing and Analysis

Targeted sequencing of specific exonic regions of selected genes based on whole-exome sequencing results was done utilizing custom amplicon sequencing. Selected genes included *NF2*, *TRAF7*, *AKT1*, *KLF4*, *SMO,* and *SMARCB1.* Genomic libraries of these selected genes were created using the TargetRichTM custom amplicon kit (Kailos Genetics). Selected genomic regions were targeted by PCR and adapters were ligated to the ends of the resulting PCR products. These libraries were amplified using barcoded primers, allowing for multiplexing. Libraries were pooled and sequenced on a version 2 Illumina MiSeq using paired-end 150 base pair reads. Sequence reads were processed using a similar bioinformatics pipeline as for the whole exome data (above). Variants were called for all samples using GATK.

Samples were prepared by Victoria Clark. Sequencing protocols were performed by YCGA. The bioinformatics pipeline and result analysis were performed by Victoria Clark.

Custom Molecular Inversion Probe Sequencing and Analysis

Additional, targeted sequencing of exonic regions and exon-intron boundaries of selected genes based on whole-exome sequencing results was done using molecular inversion probes (MIPs). Selected genes included *NF2*, *TRAF7*, *AKT1*, *KLF4*, *SMO,* and *SMARCB1.* The molecular inversion probes were designed and libraries were generated as previously described by O'Roak et al., 2012 (200), with slight modifications. Briefly, overlapping probes were designed to span the exons and exon-intron boundaries of the aforementioned selected genes. The ordered probes were synthesized by Integrated DNA Technologies, Coralville, IA. Probes were pooled equimolarly and phosphorylated. Probe hybridization was optimized via using serial dilutions of phosphorylated and pooled probes. Multiplexed DNA capture of the targeted sequences of the selected genes was performed via probe hybridization, gap filling and ligation, and exonuclease digestion. 150 ng of genomic DNA for each sample was used. The captured DNA was amplified using barcoded primers which allowed for multiplexing. Libraries were cleaned up using AMPure XP beads (Beckman Coulter, Brea, CA), quantified and 80 samples (75 experimental and 5 controls) were pooled together. Pooled libraries were sequenced on Hiseq

2500 using paired-end 101 base pair reads according to the manufacturers protocol. Sequence reads were analyzed a processed using a modified version of the bioinformatics pipeline and quality filters described above for whole-exome sequence analysis. Sequence run quality and analysis validity was assessed for each pool via analysis of the control samples. The probe design was performed by Victoria Clark. The MIPs protocol was performed by Jacob Baranoski. Pooled library sequencing was performed by YCGA. The bioinformatics pipeline was modified and sequence files were run by Victoria Clark. Sequence results were analyzed by Jacob Baranoski and Victoria Clark.

Sanger Sequencing

Coding variants detected by whole-exome, custom amplicon, and MIPs sequencing were confirmed by Sanger sequencing using standard protocols. An additional cohort of tumors was also screened for mutations within the coding regions of the *SMARCB1* gene via Sanger sequencing using standard protocols. Tumor-matched blood samples were also screened for mutations within the coding regions of the *SMARCB1* gene via Sanger sequencing using standard protocols to establish that mutations identified in tumor tissue were indeed somatic mutations. Briefly, selected exons and selected exon–intron boundaries (based on whole-exome and MIPs sequence data) of *SMARCB1* were identified using the University of California, Santa Cruz (UCSC) Genome Browser (http://genome.ucsc.edu). Unique primers

were designed using Sequencher 4.8 (Gene Codes) and synthesized by the W.M. Keck DNA Sequencing Facility at Yale School of Medicine. The selected fragments were amplified, purified and direct re-sequencing was performed using ABI's 9800 Fast Thermocyclers via polymerase chain reaction (PCR). The amplicons were analyzed on a3730xL DNA Analyser (Applied Biosystems) at the W.M. Keck DNA Sequencing Facility at Yale School of Medicine. Variants were identified using Sequencher 4.8 (Gene Codes) by comparing the sequences obtained from the tumor samples to the reference sequence as obtained from UCSC Genome Browser (http://genome.ucsc.edu). Amplification and sequencing primers were designed by Jacob Baranoski. PCRs and sample submission were preformed by Jacob Baranoski. Sequencing were performed by the W.M. Keck DNA Sequencing Facility at Yale School of Medicine. Sequence and variant analysis was performed by Jacob Baranoski.

Chromosome 22 Assessment via Q-PCR

Chromosome 22 status was assessed by quantitative real-time PCR (Q-PCR) using Fast SYBR Green Master Mix (Roche Applied Science, Indianapolis, IN, USA).
For each sample, two exons (exon 3 and exon 12) in the *NF2* gene were used for quantification and normalized against primers for two or three control chromosomes (a combination of Chr10, Chr11, and Chr16). Samples and controls were run in triplicate. Dissociation-curves were generated to ensure primer

specificity. To determine the threshold cycle, female reference DNA (Promega, Madison, WI, USA), diluted at 22ng/uL was used for 4 serial dilutions from 1/4 fold to 1/256. Each qPCR run were compared to 3 samples: a commercially available reference female DNA, DNA from a whole genome genotyped meningioma sample with known Chr22 loss, and DNA from a whole genome genotyped meningioma sample with known intact Chr22. A ratio < 0.7 was used as criteria for determining chromosomal loss. This protocol and subsequent analysis were performed by Jacob Baranoski.

Whole-Genome Genotyping

An alternative method that was also used to assess chromosome 22 status, as well as the integrity of the twenty-two other chromosomes, was whole-genome genotyping analysis. To accomplish this, the Illumina Platform was utilized. Human OmniExpress-12v1.0 BeadChips were used according to the manufacturer's protocol (Illumina, San Diego, CA, USA). Copy number variations (CNVs) were detected by comparing the normalized signal intensity between tumor and matched blood or tumor and the average of all blood samples if specific patient matched blood was not available or not genotyped. Segmentation was performed on log intensity ratios using DNACopy algorithm (201). Large-scale chromosomal deletion or amplification was defined as affecting more than one-third of the chromosomal arm with accompanying log ratio of signal intensities < -0.1 or > 0.1, and B allele

frequencies (BAF) at heterozygous sites deviating from 0.5 by at least 0.05 units. Large-scale copy neutral LOH was defined similarly, with the exception of log ratio of signal intensities being between -0.1 and 0.1. Sample preparation was performed by Jacob Baranoski and Victoria Clark. Genotyping chips were sequenced by YCGA. Log intensity ratios were calculated by Akdes Serrin. Result analyses were performed by Akdes Serrin, Jacob Baranoski, and Victoria Clark.

RNA Expression Analysis

To determine the levels of relative gene expression in tumor samples, Illumina HumanHT12.v4 gene expression microarray chips were used. RNA Integrity Number (RIN) analysis was first performed to ensure adequate RNA quality. Extracted tumor RNA samples were placed on Agilent RNA Nano Chips (Agilent Technologies, Santa Clara, CA). These samples were then analyzed on Agilent 2100 Bioanalyzer using the manufacture's protocol and software (Agilent Technologies, Santa Clara, CA). Samples with RINs less than 7 were excluded from further analysis.

Data from the Illumina HumanHT12.v4 gene expression microarray chips for samples that passed quality control metrics were used to perform an unsupervised hierarchical clustering using the euclidean distance as the dissimilarity metric and the average agglomerative method for clustering. Differential gene expression analysis was then performed using the log-odds of differential expression value as

implemented in the *ebayes* method of the *limma R* package. Tumor samples were compared to tumors with other driver mutations and also to normal adult and embryologic meningeal tissue. RIN analysis was performed by Jacob Baranoski. Sample preparation was performed by Jacob Baranoski and Victoria Clark. Expression microarray protocol was performed by YCGA. Unsupervised hierarchical clustering were performed by Akdes Serrin. Comparative analyses were performed by Akdes Serrin and Jacob Baranoski.

RESULTS

Identification of *SMARCB1*-Mutant Meningiomas

Whole-Exome and Custom Amplicon Sequencing

Whole-exome sequencing performed on a discovery cohort of meningiomas (n=50) identified two tumors with somatic *SMARCB1* mutations. The first tumor, designated MUN-MN-301, harbored a point mutation in an exon of the *SMARCB1* gene (Chr22: 24176339; G>A), which resulted in a R386H amino acid substitution. The second meningioma, MUN-MN-295, was identified to harbor a single base pair deletion (Chr22: 24175813del; AC>A), resulting in a frameshift mutation. Each of these tumors was also found to possess a concurrent somatic mutation in the *NF2* gene. MUN-MN-301 possessed a single base pair insertion in the *NF2* gene (Chr22: 30032748ins; G>GA) resulting in a frameshift mutation. MUN-MN-295 also harbored a frameshift mutation in the *NF2* gene (Chr22: 30035146del; AGAATGCT>A).

A replication cohort of meningiomas (n=262) was then analyzed via custom amplicon sequencing. Amplicon sequencing identified an additional five meningiomas with somatic *SMARCB1* mutations. Interestingly, four of these five tumors were found to harbor the identical mutation as was discovered in MUN-MN-301 – R386H. The fifth tumor possessed a single base pair mutation resulting in an

amino acid substitution at a neighboring location – R383Q. These data are summarized in Table 1.

Table 1. *SMARCB1* Mutations Identified via Whole-Exome and Custom Amplicon Sequencing

Tumor Sample	**Sequencing Method**	***SMARCB1* Mutation**	***SMARCB1* Mutation Consequence**
MUN-MN-295	Whole-Exome	Chr22:24175813_AC>A	Frameshift
MUN-MN-301	Whole-Exome	Chr22:24176339_G>A	R386H
MSK-MN-500	Amplicon	Chr22:24176339_G>A	R386H
MSK-MN-584	Amplicon	Chr22:24176330_G>A	R383Q
MSK-MN-845-1	Amplicon	Chr22:24176339_G>A	R386H
MUN-MN-263	Amplicon	Chr22:24176339_G>A	R386H
MUN-MN-56	Amplicon	Chr22:24176339_G>A	R386H

Molecular Inversion Probe Sequencing

The identification of *SMARCB1* mutations via whole-exome and amplicon sequencing prompted further investigation of this gene in meningiomas. Molecular inversion probes (MIPs) were designed to analyze the coding regions of the *SMARCB1* and *NF2* genes (as well as *TRAF7*, *KLF4*, *AKT1*, and *SMO*) based on the whole-exome sequencing results. A cohort of 436 previously unanalyzed meningiomas of various grades and locations were sequenced using MIPs sequencing. Seventeen of these meningiomas were identified as having *SMARCB1* mutations. Thirteen of these 17 tumors harbored the R386H *SMARCB1* mutation identified in the whole-exome and amplicon sequenced cohorts; 2 were found to

harbor the R383Q *SMARCB1* mutation identified in one of the amplicon sequenced tumors; 2 were found to have frameshift mutations. Of these 17 meningiomas found to harbor *SMARCB1* mutations, 12 were identified by MIPs sequencing to have concurrent mutations affecting the coding region of *NF2.* In addition to these 17 meningiomas, a single tumor (YALE-1205) was identified to have a *SMARCB1* R386H mutation via Sanger sequencing screening (n=24). These data are summarized in Table 2.

Table 2. *SMARCB1* Mutations Identified via MIPs Sequencing and Sanger Screening

Tumor Sample	**Sequencing Method**	***SMARCB1* Mutation**	***SMARCB1* Mutation Consequence**
BONN-T-1075	MIPs	Chr22:24176339_G>A	R386H
BONN-T-1215	MIPs	Chr22:24176339_G>A	R386H
BONN-T-1797	MIPs	Chr22:24176339_G>A	R386H
BONN-T-2102	MIPs	Chr22:24176339_G>A	R386H
BONN-T-2108	MIPs	Chr22:24176339_G>A	R386H
BONN-T-2296	MIPs	Chr22:24176339_G>A	R386H
BONN-T-2432	MIPs	Chr22:24176339_G>A	R386H
BONN-T-2758	MIPs	Chr22:24176339_G>A	R386H
BONN-T-314	MIPs	Chr22:24176330_G>A	R383Q
BONN-T-3991	MIPs	Chr22:24176330_G>A	R383Q
BONN-T-4136	MIPs	Chr22:24176339_G>A	R386H
BONN-T-439	MIPs	Chr22:24176339_G>A	R386H
BONN-T-841	MIPs	Chr22:24176339_G>A	R386H
BONN-T-847	MIPs	Chr22:24175835_ACT>A	Frameshift
KOLN-HT-2835	MIPs	Chr22:24175835_ACT>A	Frameshift
KOLN-HT-3369	MIPs	Chr22:24176339_G>A	R386H
YALE-251	MIPs	Chr22:24176339_G>A	R386H
BONN-T-1205	Sanger Screening	Chr22:24176339_G>A	R386H

Sanger Confirmations of SMARCB1 Mutations and Verification as Somatic Variants

The 24 meningiomas identified as being *SMARCB1*-mutant via whole-exome, amplicon, and MIPs sequencing underwent subsequent Sanger sequencing to confirm the called *SMARCB1* variants. All 24 variants were successfully confirmed via Sanger sequencing. Figure 2a is a representative chromatogram demonstrating Sanger sequencing confirmation of a heterozygous *SMARCB1* mutation in meningioma tissue.

Figure 2.

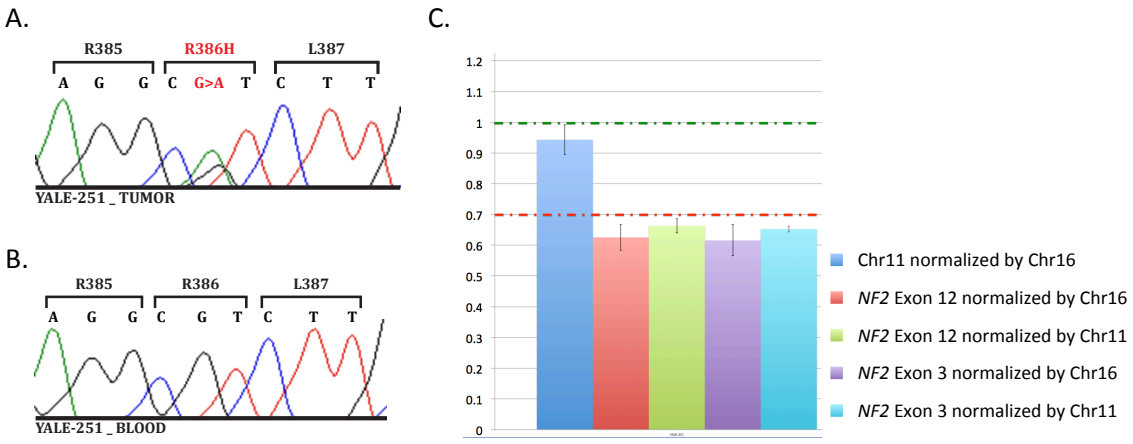

Figure 2. *SMARCB1*-Mutant Meningiomas Harbor Somatic *SMARCB1* Mutations in an *NF2*-Mutant Background

A.) Representative chromatogram demonstrating Sanger confirmation of the heterozygous *SMARCB1* R386H variant in the tumor tissue from subject YALE-251. Similar chromatograms were obtained for the other 23 meningiomas identified as being *SMARCB1*-mutant via whole-exome, custom amplicon, and MIPs sequencing – all identified *SMARCB1* variants were successfully Sanger confirmed.

B.) Representative chromatogram demonstrating Sanger screening of the *SMARCB1* gene in the germline DNA obtained from white blood cells for subject YALE-251. Note that the G>A substitution that results in the R386H variant that was present in the tumor tissue for subject YALE-251 is not present in the germline DNA. This verified that *SMARCB1* mutation was a somatic mutation. Similar chromatograms were obtained for the other 9 subjects for which germline DNA was available. All *SMARCB1* variants screened were identified as somatic mutations.

C.) Representative results of *NF2* q-PCR analysis for subject YALE-251 demonstrating *NF2*-loss. Two exons (3 and 12) of *NF2* were quantified relative to control exons on chromosomes 11 and 16. A ratio of <0.7 was utilized as the cut off for deletion (ratio determined by pilot data utilizing whole-genome genotyping results). Similar results demonstrating *NF2*-loss were obtained for the other *SMARCB1*-mutant tumors screened via q-PCR. All 25 *SMARCB1*-mutant meningiomas were found to harbor concurrent mutations in *NF2* and/or concurrent *NF2*-loss / Chr22-loss.

Subject blood samples were available for 10 of the 25 meningiomas identified harboring *SMARCB1* mutations. DNA obtained from the white blood cells of these patients underwent Sanger sequencing screening for the *SMARCB1* mutations identified in the respective paired tumor samples. None of the *SMARCB1* mutations identified in the tumor samples were present in the DNA obtained from the respective patient's white blood cells, indicating that the *SMARCB1* variants present in the meningiomas are indeed somatic mutations. See Figure 2b. These data are summarized in Table 3.

Table 3. Results of Somatic Assessment of *SMARCB1* Variants

Tumor Sample	***SMARCB1* Mutation in Tumor**	***SMARCB1* Gene Status in Subject's Germline DNA**
BONN-T-1797	R386H	Wildtype
BONN-T-2758	R386H	Wildtype
BONN-T-314	R383Q	Wildtype
BONN-T-439	R386H	Wildtype
BONN-T-841	R386H	Wildtype
MSK-MN-584	R383Q	Wildtype
MSK-MN-845-1	R386H	Wildtype
MUN-MN-295	Frameshift (Chr22:24175813_AC>A)	Wildtype
MUN-MN-301	R386H	Wildtype
YALE-251	R386H	Wildtype

SMARCB1-Mutant Meningiomas Represent a Distinct Subset of *NF2*-Mutant Meningiomas

Somatic SMARCB1 Mutations with Concurrent NF2 Mutations and/or Chr22 Loss

In addition to identifying *SMARCB1* mutations, whole-exome, custom amplicon, and MIPs sequencing technologies were used to identify coding mutations affecting the *NF2* gene. Likewise, whole-genome genotyping and Q-PCR analyses were conducted to identify chromosome 22 (Chr22) and *NF2* gene deletion, respectively.

As in the two tumors that had *SMARCB1* mutations identified via whole-exome sequencing, all five of the *SMARCB1*-mutant tumors identified via amplicon sequencing were also found to possess concurrent mutations in *NF2* and/or concurrent *NF2*-loss / Chr22-loss (determined via genotyping and/or *NF2* Q-PCR analyses).

Similarly, all 17 *SMARCB1*-mutant meningiomas identified via MIPs sequencing and the one *SMARCB1*-mutant tumor identified via Sanger screening were also found to possess concurrent mutations in *NF2* and/or concurrent deletion of Chr22 or *NF2* (determined via genotyping and/or *NF2* Q-PCR analyses). See Figure 2c. These data are summarized in Table 4.

Table 4. Concurrent *NF2* / Chr22 Aberrations Identified in *SMARCB1*-Mutant Meningiomas

Tumor Sample	Sequencing Method	*SMARCB1* Mutation	*NF2* Status	*NF2* Mutation
BONN-T-1075	MIPs	R386H	*NF2*-mutant	Chr22:30032805_G>A
BONN-T-1205	Sanger Screening	R386H	*NF2*-loss	n/a
BONN-T-1215	MIPs	R386H	Chr22q-loss	n/a
BONN-T-1797	MIPs	R386H	*NF2*-mutant	Chr22:30051666_G>T
BONN-T-2102	MIPs	R386H	*NF2*-loss & *NF2*-mutant	Chr22:30038219_TC>T
BONN-T-2108	MIPs	R386H	*NF2*-loss & *NF2*-mutant	Chr22:30032794_C>T
BONN-T-2296	MIPs	R386H	Chr22q-loss	n/a
BONN-T-2432	MIPs	R386H	*NF2*-mutant	Chr22:30057330_T>C
BONN-T-2758	MIPs	R386H	*NF2*-mutant	Chr22:30035201_G>C ; Chr22:30067867_G>A
BONN-T-314	MIPs	R383Q	Chr22q-loss & *NF2*-mutant	Chr22:30074265_CA>C
BONN-T-3991	MIPs	R383Q	Chr22q-loss	n/a
BONN-T-4136	MIPs	R386H	Chr22q-loss & *NF2*-mutant	Chr22:30067938_G>T
BONN-T-439	MIPs	R386H	*NF2*-mutant	Chr22:30057326_GA>G
BONN-T-841	MIPs	R386H	Chr22q-loss	n/a
BONN-T-847	MIPs	Frameshift (Chr22:24175835_ACT>A)	*NF2*-mutant	Chr22:30057329_G>A
KOLN-HT-2835	MIPs	Frameshift (Chr22:24175835_ACT>A)	*NF2*-mutant	Chr22:30051639_G>A
KOLN-HT-3369	MIPs	R386H	*NF2*-mutant	Chr22:30032854_ATGGA>A
MSK-MN-500	Amplicon	R386H	*NF2*-loss & *NF2*-mutant	Chr22:30067836_C>T
MSK-MN-584	Amplicon	R383Q	*NF2*-loss & *NF2*-mutant	Chr22:30057302_C>T
MSK-MN-845-1	Amplicon	R386H	*NF2*-loss & *NF2*-mutant	Chr22:30051639_G>A
MUN-MN-263	Amplicon	R386H	*NF2*-loss	n/a
MUN-MN-295	Whole-Exome	Frameshift (Chr22:24175813_AC>A)	Chr22q-loss	n/a
MUN-MN-301	Whole-Exome	R386H	Chr22q-loss	n/a
MUN-MN-56	Amplicon	R386H	Chr22q-loss	n/a
YALE-251	MIPs	R386H	*NF2*-loss	n/a

Whole-genome genotyping was also used to assess the stability of all 23 chromosomes for some of these tumors. The genomes of the *SMARCB1*-mutant meningiomas appear relatively stable. Only 2 of the 10 tumors that underwent whole-genome genotyping analysis demonstrated any large-scale chromosomal events aside from chromosome 22q loss. When examining the chromosomal stability of 4 high-grade *SMARCB1*-mutant meningiomas analyzed, only one had any large-scale events aside from chromosome 22q loss. These data are summarized in Table 5. Interestingly, this stability is in contrast to the usual finding of widespread chromosomal instability in high-grade tumors. For example, 24 of 26 non-*SMARCB1*-mutant *NF2*-mutant / Chr22-loss high-grade meningiomas in our database had large-scale chromosomal alterations (and/or numerous focal events) in addition to Chr22q loss. These data are summarized in Appendix Table 1.

Table 5. Whole-Genome Genotyping Results for *SMARCB1*-Mutant Meningiomas

Tumor Sample	*SMARCB1* Mutation	Tumor Grade	Large-Scale Chr Deletion Events	Focal Chr Deletion Events	Large-Scale Chr Amp. Events	Focal Chr Amp. Events	Large-Scale Chr LOH Events	Focal Chr LOH Events
BONN-T-1215	R386H	1	8p / 8q / 22q	None	None	None	None	None
BONN-T-2296	R386H	1	22q	16p / 19p	None	None	None	None
BONN-T-314	R383Q	2	22q	None	None	None	None	None
BONN-T-3991	R383Q	1	22q	19p	None	None	None	None
BONN-T-4136	R386H	1	22q	None	None	None	None	None
BONN-T-841	R386H	2	22q	None	None	None	None	None
KOLN-HT-2835	Frameshift	2	22q	None	None	None	None	None
MUN-MN-295	Frameshift	2	22q	None	8p	None	None	None
MUN-MN-301	R386H	1	22q	None	None	None	None	None
MUN-MN-56	R386H	1	22q	16p / 20q	None	None	None	3p / 12p / 12q

Chr = Chromosomal Amp. = Amplification LOH = Loss of heterozygosity

Expression Profile of SMARCB1-Mutant Meningiomas

To further characterize these *SMARCB1*-mutant meningiomas, we performed gene expression analysis. Unsupervised hierarchical clustering analysis based on meningioma gene expression data demonstrated that the expression profiles of *SMARCB1*-mutant meningiomas cluster similarly to other *NF2*-mutant/Chr22 loss meningiomas. That is, the expression profiles of these tumors are distinctly different from the expression profiles of meningiomas that do not harbor concurrent *NF2* mutations (*TRAF7/AKT1*-mutant meningiomas, for example). However, within this family, *SMARCB1*-mutant meningiomas cluster as distinct subgroups. See Figure 3.

Figure 3.

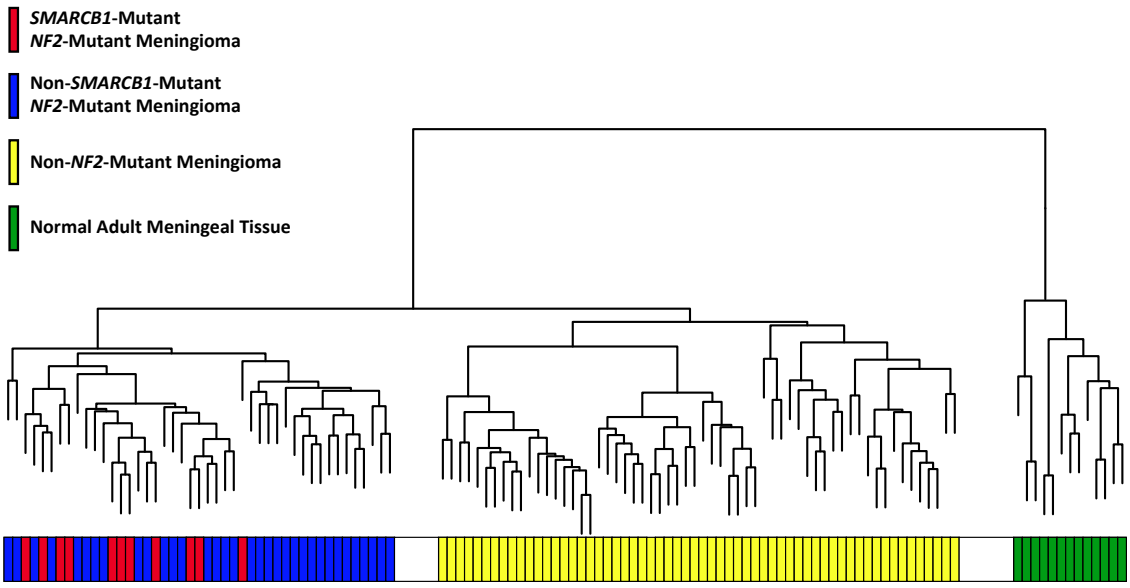

Figure 3. Unsupervised Hierarchal Clustering Analysis of Meningioma Gene Expression

Unsupervised hierarchal clustering results of gene expression analysis for meningiomas. Each terminal branch of the graph (and associated bar) represents a single tissue sample. The more closely clustered the terminal branches, the more similar the samples are; expression profiles of tissues that are dissimilar have branches further apart. Each color bar represents a different tissue type – red is *SMARCB1*-mutant meningiomas; blue is non-*SMARCB1*-mutant *NF2*-mutant meningiomas; yellow is non-*SMARCB1*, non-*NF2* mutant meningiomas; green is normal adult meningeal control tissue. Meningiomas, as a whole, demonstrate a very distinct gene expression profile from that of normal adult meningeal tissue (as evident by the divergent branching pattern at the earliest point in the tree). Within the meningiomas, *NF2*-mutant and non-*NF2* mutant meningiomas exhibit very distinct expression profiles. Within the *NF2*-mutant meningioma superfamily, note that *SMARCB1*-mutant tumors appear to form a unique subgroup that is distinct from the majority of non-*SMARCB1*-mutant *NF2*-mutant meningiomas.

Increased Expression of GLI1 and EZH2 Contribute to Differential Clustering of SMARCB1-Mutant Meningiomas within the NF2-Mutant Meningioma Superfamily

To investigate the factors that account for this distinct clustering within the *NF2* superfamily, we performed differential gene expression analysis. We sought to determine which genes were either more or less expressed in these *SMARCB1*-mutant meningiomas compared to other *NF2*-mutant (but non-*SMARCB1*-mutant) meningiomas, non-*NF2*-mutant meningiomas, and normal adult meningeal tissue as a control.

The top two differentially over-expressed genes in *SMARCB1*-mutant meningiomas compared to non-*SMARCB1*-mutant *NF2*-mutant meningiomas were *SCG2* and *RSPO3*.

SCG2 codes for the protein secretogranin II. Secretogranin II is thought be involved in the packaging of neuropeptides into secretory vesicles (202, 203). Secretogranin II can be cleaved to an active form called Secretoneurin (204). Previous studies have found increased *SCG2* expression in other tumor types (205) and secretogranin II has also been shown to inhibit apoptosis by blocking caspase-3 activation (206). *SCG2* expression in *SMARCB1*-mutant meningiomas was also increased when compared to *SCG2* expression levels in normal control meningeal tissue.

RSPO3 codes for the protein R-spondin 3, which is a secreted protein known to regulate beta-catenin (CTNNB1) (207). *RSPO3* fusions have been previously associated with a subset of colon cancer (208) and increased *RSPO3* expression has been demonstrated in other cancer types (209). *RSPO3* expression in *SMARCB1*-mutant meningiomas was also found to be increased when compared to *RSPO3* expression levels in normal control meningeal tissue.

The top differentially under-expressed gene that has previously been associated with tumorigenesis in *SMARCB1*-mutant meningiomas compared to non-*SMARCB1*-mutant *NF2*-mutant meningiomas was *IGFBP3. IGFBP3* codes for the protein Insulin-like growth factor-binding protein 3 (IGFBP-3). IGFBP-3 is capable of binding IGF-1 and IGF-2 and preventing these ligands from binding to their receptor IGF1R (210, 211). *IGFBP3* is also considered to be a tumor suppressor gene; down-regulation of *IGFBP3* has previously been associated with numerous tumor types (212-214). *IGFBP3* expression in *SMARCB1*-mutant meningiomas was also decreased when compared to *IGFBP3* expression levels in normal control meningeal tissue.

We next examined the relative expression levels of genes known to interact with *SMARCB1* and be involved in tumorigenesis. These genes included *MYC, CDKN2A, CCND1, GLI1,* and *EZH2*.

Consistent with the previously reported interactions between *SMARCB1* and *MYC*, *MYC* expression was decreased in *SMARCB1*-mutant meningiomas compared to non-

SMARCB1-mutant *NF2*-mutant meningiomas. Interestingly, however, *MYC* expression in *SMARCB1*-mutant meningiomas was not decreased when compared to *MYC* expression levels in normal control meningeal tissue.

Similarly, consistent with the previously reported interactions between *SMARCB1* and *CDKN2A*, *CDKN2A* expression was decreased in *SMARCB1*-mutant meningiomas compared to non-*SMARCB1*-mutant *NF2*-mutant meningiomas. Again, however, *CDKN2A* expression in *SMARCB1*-mutant meningiomas was not decreased when compared to *CDKN2A* expression levels in normal control meningeal tissue.

CCND1 levels were not directly assessed, however, the expression of other members of the cyclin-D family (*CCND2* and *CCND3*) were analyzed. Both *CCND2* and *CCND3* expression levels were increased in *SMARCB1*-mutant meningiomas compared to non-*SMARCB1*-mutant *NF2*-mutant meningiomas – this is what would be expected for *CCND1* based on previously reported interactions between *SMARCB1* and *CCND1*. Both *CCND2* and *CCND3* expression levels were also increased in *SMARCB1*-mutant meningiomas when compared to *CCND2* and *CCND3* expression levels in normal control meningeal tissue.

The next gene analyzed was *GLI1*, a member of the sonic hedgehog pathway. *GLI1* expression was markedly increased in *SMARCB1*-mutant meningiomas compared to other *NF2*-mutant meningiomas that did not harbor concurrent *SMARCB1* mutations. Interestingly, the *GLI1* expression profile of these *SMARCB1*-mutant

meningiomas more closely resembled that of *SMO*-mutant meningiomas that were previously described by Clark et al. as tumors of the midline anterior skull base. *GLI1* expression in *SMARCB1*-mutant meningiomas was also increased when compared to *GLI1* expression levels in normal control meningeal tissue.

The final gene analyzed was *EZH2*, which codes for a member of the Polycomb-group protein family and is involved in chromatin remodeling. *EZH2* expression was increased in *SMARCB1*-mutant meningiomas compared to other *NF2*-mutant meningiomas that did not harbor concurrent *SMARCB1* mutations. *EZH2* expression in *SMARCB1*-mutant meningiomas was also increased when compared to *EZH2* expression levels in normal control meningeal tissue. Expression data are summarized in Table 6.

Table 6. Differential Gene Expression Results

Gene	Mean *SMARCB1*-Mutant Meningioma Expression	Mean Non-*SMARCB1*-Mutant *NF2*-Mutant Meningioma Expression	Mean Normal Adult Meningeal Tissue Expression	Difference Between *SMARCB1*-Mutant and Non-*SMARCB1*-Mutant *NF2*-Mutant Meningiomas	Difference Between *SMARCB1*-Mutant Meningioma and Normal Adult Meningeal Tissue
SCG2	10.529	8.097	5.854	2.432	4.675
RSPO3	9.684	7.328	4.593	2.356	5.091
IGFBP3	7.323	8.869	11.905	-1.546	-4.582
MYC	7.577	7.878	5.479	-0.301	2.098
CDKN2A	4.978	5.189	4.778	-0.212	0.200
CCND2	9.170	8.874	8.860	0.296	0.310
CCND3	10.243	9.890	9.639	0.353	0.605
GLI1	6.169	5.329	4.775	0.840	1.394
EZH2	5.086	4.929	4.487	0.156	0.599

The differential expression of these genes contributes to the distinct clustering of the *SMARCB1*-mutant meningiomas within the *NF2*-mutant superfamily. A list of the top 300 differentially expressed (top 150 up-regulated and top 150 down-regulated) genes between *SMARCB1*-mutant and non-*SMARCB1*-mutant *NF2*-mutant meningiomas are listed in Appendix Table 2.

SMARCB1-Mutant Meningiomas Are Midline Convexity Tumors with an Increased Predilection to Be *De Novo* High-Grade Lesions

We sought to determine if the genomic differences identified in *SMARCB1*-mutant meningiomas correlated with distinctions in clinical presentation. Demographic and clinical data for these patients are summarized in Table 7. Of the 25 patients with meningiomas 20 were female (80%). The median age at time of surgery was 64 years. Among these 25 meningiomas, no specific low-grade histological subtype was significantly more prevalent.

Table 7. Demographic and Clinical Data for *SMARCB1*-Mutant Meningioma Patients

Tumor Sample	*SMARCB1* Mutation	Patient Age	Patient Gender	Tumor Grade	Tumor Histology	General Location	Specific Location	Midline Location?
BONN-T-1075	R386H	51	F	1	Transitional	Convexity	Frontal	Non-midline
BONN-T-1205	R386H	73	F	1	Transitional	ASB	Olfactory Groove	Midline
BONN-T-1215	R386H	75	F	1	Transitional	ASB	Frontobasal	Midline
BONN-T-1797	R386H	64	F	1	Fibrous	Spinal	T2	n/a
BONN-T-2102	R386H	56	F	1	Transitional	Convexity	Parafalcine	Midline
BONN-T-2108	R386H	73	F	1	Transitional	Convexity	Parasagittal	Midline
BONN-T-2296	R386H	68	F	1	Psammomatous	ASB	Frontobasal	Midline
BONN-T-2432	R386H	61	F	1	Meningothelial	Convexity	Parasagittal	Midline
BONN-T-2758	R386H	65	M	2	Meningothelial	Other	Petrous Bone	Lateral
BONN-T-314	R383Q	49	F	2	Fibrous	Convexity	Parasagittal	Midline
BONN-T-3991	R383Q	66	F	1	Transitional	Convexity	Parafalcine	Midline
BONN-T-4136	R386H	61	F	1	Fibrous	Convexity	Parafalcine	Midline
BONN-T-439	R386H	72	M	2	Atypical	Convexity	Tentorial	Non-midline
BONN-T-841	R386H	67	M	2	Atypical	Convexity	Parafalcine	Midline
BONN-T-847	Frameshift	59	F	2	Atypical	Convexity	Parafalcine	Midline
KOLN-HT-2835	Frameshift	73	M	2	n/a	ASB	Olfactory Groove	Midline
KOLN-HT-3369	R386H	61	M	1	Meningothelial	ASB	Olfactory Groove	Midline
MSK-MN-500	R386H	64	F	2	Atypical	Convexity	Frontal	Non-midline
MSK-MN-584	R383Q	54	F	1	n/a	Convexity	Parafalcine	Midline
MSK-MN-845-1	R386H	81	F	1	n/a	MSB	Lateral Sphenoid Wing	Lateral
MUN-MN-263	R386H	58	F	1	LPMR	Convexity	Parasagittal	Midline
MUN-MN-295	Frameshift	70	F	2	atypical	Convexity	General	Non-midline
MUN-MN-301	R386H	58	F	1	Psammomatous	Convexity	Parafalcine	Midline
MUN-MN-56	R386H	51	F	1	Transitional	CPA	CPA	Lateral
YALE-251	R386H	29	F	2	n/a	Convexity	Parafalcine	Midline

Patient age is in years

ASB = anterior skull base

CPA = cerebellopontine angle

LPMR = Lymphoplasmacyte-rich

MSB = middle skull base

T2 = 2nd thoracic vertebrae

Interestingly, *SMARCB1*-mutant meningiomas appeared to have a slight predilection to being high-grade at time of surgery. Nine of the 25 (36%) were diagnosed as *de novo* high-grade lesions. This is a markedly higher percentage than reported in the literature (~20%) (5-7). Further, as noted above, these high-grade *SMARCB1*-mutant meningiomas appear to possess markedly increased chromosomal stability compared to non-*SMARCB1*-mutant *NF2*-mutant high-grade meningiomas. Neither median patient age at time of surgery nor gender predominance for high-grade *SMARCB1*-mutant meningiomas (65 years; 55% female) differed significantly from those of non-*SMARCB1*-mutant *NF2*-mutant high-grade meningiomas (62 years; 54% female). These data are summarized in Appendix Table 3.

We sought to identify a "mutation map" for *SMARCB1*-mutant meningiomas. Lesion location information was available for all 25 *SMARCB1*-mutant meningiomas. 24 of these 25 (96%) meningiomas were intracranial tumors; one was a spinal meningioma occurring at level T2. Of the 24 intracranial tumors, 16 (67%) were convexity lesions and 5 (21%) were anterior skull base meningiomas.

Interestingly, when examining the intracranial convexity meningiomas, 12 of the 16 (75%) were midline tumors – 8 parafalcine and 4 parasagittal. Similarly, when looking at the *SMARCB1*-mutant meningiomas that formed along the anterior skull base, all 5 tumors (100%) were midline – 3 formed along the olfactory groove and 2 were described as frontobasal lesions. Overall, of the 24 known intracranial meningiomas, 17 (71%) originated along the midline. See Figure 4. Taken together,

these data suggest that *SMARCB1*-mutant meningiomas are predominantly midline tumors with a slightly increased predilection to be high-grade at time of diagnosis.

Figure 4.

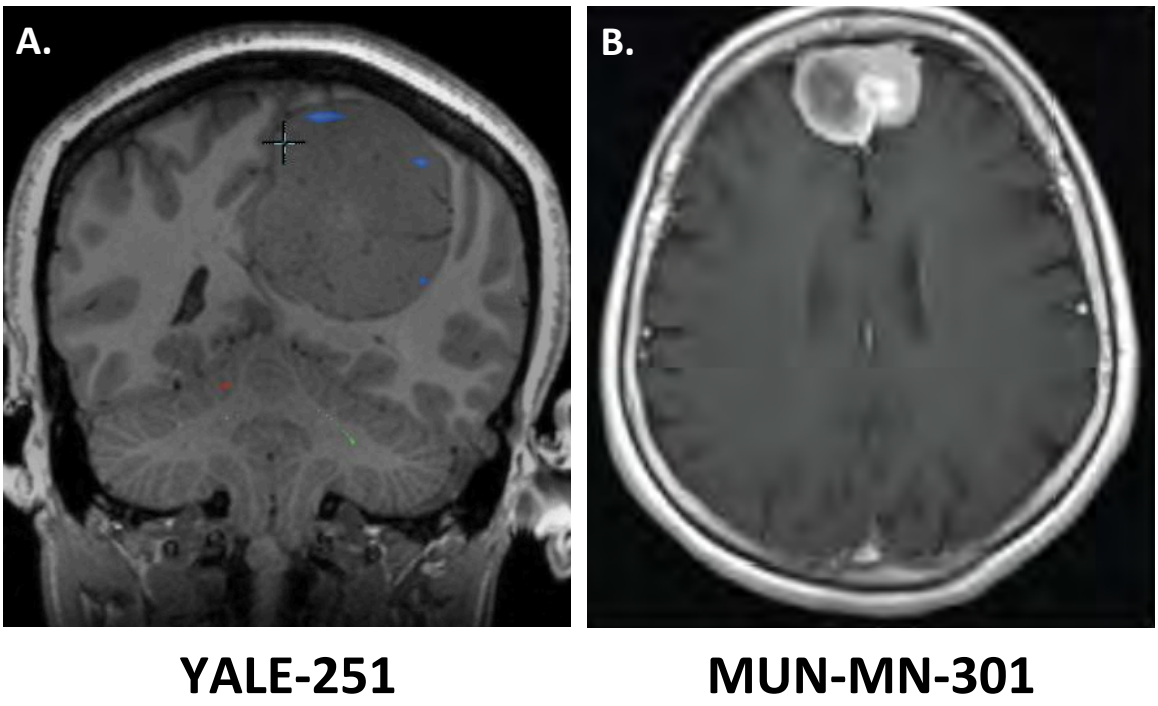

Figure 4. *SMARCB1*-Mutant Meningiomas Are Midline Convexity Lesions

Representative pre-operative MRI images of two *SMARCB1*-mutant meningiomas, YALE-251 (A.) and MUN-MN-301 (B.). Note the midline location of these lesions. Both of these meningiomas are parasagittal tumors. Similar MRI images and/or radiology reports detailing the location of all 25 *SMARCB1*-mutant meningiomas were analyzed.

DISCUSSION

Genetics of *SMARCB1*-Mutant Meningiomas

Here, we identified 25 meningiomas that harbored somatic *SMARCB1* mutations (772 meningiomas were analyzed in total). These tumors represent a genetically and phenotypically distinct subgroup of *NF2*-mutant / Chr22-loss meningiomas. The somatic *SMARCB1* mutations we identified can be categorized as one of three types. The first two are recurrent point mutations affecting either amino acid 386 (R386H) or amino acid 383 (R383Q) of the SMARCB1 peptide; the third category constitutes frameshift mutations. All 25 meningiomas with somatic SMARCB1 mutations also possessed concurrent somatic *NF2*-mutaitons and/or somatic Chr22-loss.

RNA expression hierarchical clustering analysis demonstrated that *SMARCB1*-mutant meningiomas cluster within the *NF2*-mutant superfamily (distinct from the non-*NF2*-mutant meningiomas); however, these tumors appear to possess a distinct expression pattern that differentiates them from non-*SMARCB1*-mutant *NF2*-mutant meningiomas. This sub-group clustering pattern is due at least in part to increased *GLI1* and *EZH2* expression in *SMARCB1*-mutant meningiomas.

GLI1 is important effector of the hedgehog pathway (183). *GLI1* expression levels in *SMARCB1*-mutant meningiomas more closely resemble those in *SMO*-mutant meningiomas that were previously identified to drive tumorigenesis of meningiomas of the olfactory groove (midline structure of the anterior skull base)

(101). Expression levels of *EZH2*, a Polycomb-group protein involved in epigenetic modification (121, 195), were also increased in *SMARCB1*-mutant meningiomas compared to non-*SMARCB1*-mutant *NF2*-mutant meningiomas.

Whole-genome genotyping analysis demonstrated that *SMARCB1*-mutant meningiomas are largely chromosomally stable – only 2 out of the 10 analyzed demonstrated a large-scale chromosomal deletion or amplification aside from Chr22q-loss. Interestingly, this holds true even for the high-grade *SMARCB1*-mutant meningiomas analyzed. Across various tumor types, chromosomal instability is traditionally considered a hallmark of high-grade lesions. However, of the 4 high-grade, *SMARCB1*-mutant meningiomas we analyzed, only one (25%) possessed any large-scale chromosomal events (MUN-MN-295 had a large-scale Chr8p amplification) aside from Chr22q-loss; no focal chromosomal aberrations were identified in these 4 samples. For comparison, 29 of 32 non-*SMARCB1*-mutant *NF2*-mutant high-grade meningiomas in our database possessed large-scale chromosomal alterations (and/or numerous focal events) in addition to Chr22q-loss.

Clinical Characteristics of *SMARCB1*-Mutant Meningiomas

Paralleling the genetic data, *SMARCB1*-mutant tumors also appear to constitute a distinct phenotypic sub-group of *NF2*-mutant meningiomas. Both the age at surgical

intervention (median = 64 years) and female predominance (20 / 25; 80%) in our cohort are in accordance with the demographics previously reported (1). The majority of concurrently *SMARCB1*-mutant meningiomas (67%) were identified in areas previously associated with *NF2*-mutatant meningiomas – convexity, spinal cord, and cerebellopontine angle (101). However, *SMARCB1*-mutant meningiomas demonstrated a strong tendency to form along the midline. Seventy-one percent of the *SMARCB1*-mutant meningiomas were identified as parasagittal or parafalcine convexity tumors or as occurring along the midline of the anterior skull base. Therefore, similarly to the mutation-location correlations described by Clark et al. for anterior skull base meningiomas, a "mutation map" for convexity lesions also appears to exist (101). In addition to the anterior-posterior *TRAF7* – *NF2* mutation gradient (described by Clark et al. and replicated in this study), a lateral-medial-lateral "map" for *SMARCB1*-mutant tumors also exists. See Figure 5. Additionally, *SMARCB1*-mutant meningiomas demonstrated an increased propensity be diagnosed as high-grade lesions at time of initial resection (36%) compared to data previously reported data (5-7).

Figure 5.

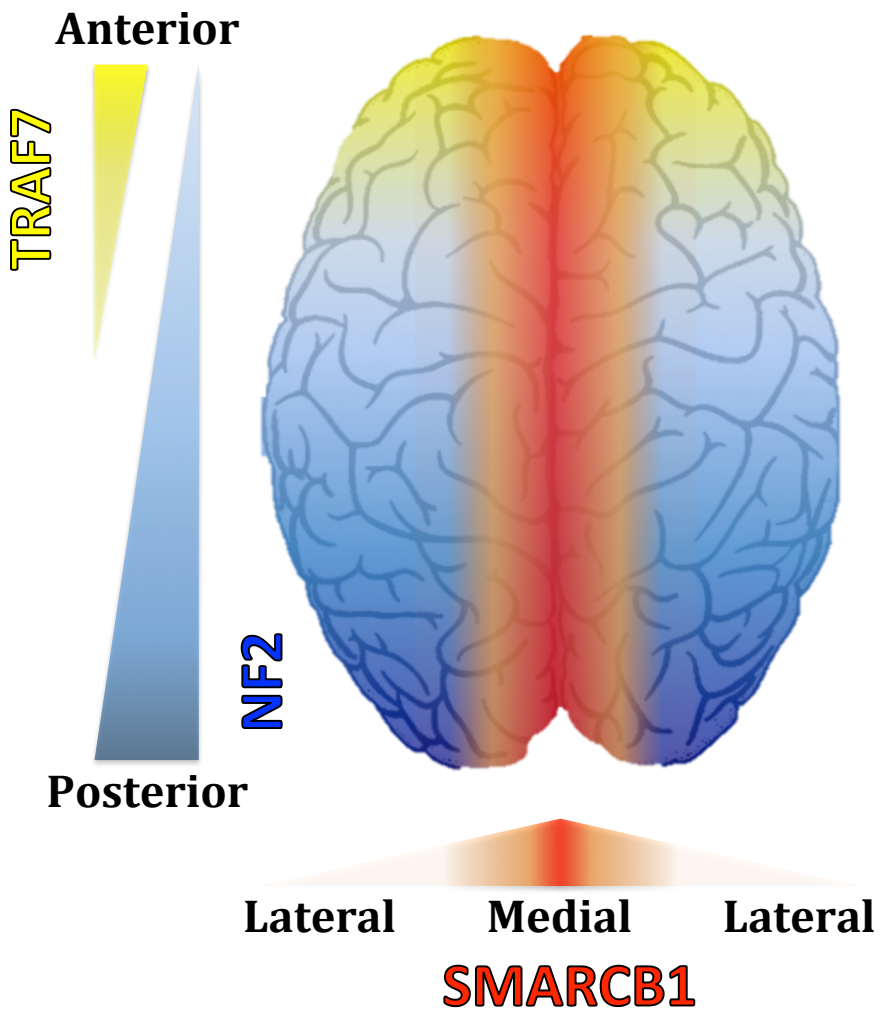

Figure 5. "Mutation-Map" for Convexity Meningiomas

A multi-tiered mutation-location gradient appears to exist for convexity meningiomas. Posterior meningiomas tend to harbor *NF2*-mutations and/or *NF2* / Chr22-loss while *TRAF7*-mutant convexity meningiomas appear to be predominantly anteriorly – this observation was first reported by Clark et al. and was replicated in this study. Additionally, a lateral-medial-lateral lesion gradient also exists with respect to *SMARCB1* mutations. *SMARCB1*-mutant meningiomas are predominantly midline lesions and also demonstrate an increased propensity to be high-grade upon initial resection.

Genetic-Clinical Correlates for *SMARCB1*-Mutant Meningiomas

Aberrant Hedgehog Signaling and Midline Tumor Location

We found that the majority of *SMARCB1*-mutant meningiomas were midline tumors. Interestingly, we also found that *SMARCB1*-mutant meningiomas demonstrated increased *GLI1* expression relative to both normal meningeal control tissue and non-*SMARCB1*-mutant *NF2*-mutant meningiomas. GLI1 is an important effector of the Hedgehog pathway and plays key roles during embryogenesis, especially with the development and patterning of midline structures (174, 175, 183). These findings are consistent with data previously published demonstrating that that the SWI/SNF complex, and the SMARCB1 component specifically, interact with the Hedgehog pathway via GLI1 (183-185). Similarly to our results, this study found that loss of *SMARCB1* resulted in aberrant upregulation of the Hedgehog pathway and increased *GLI1* expression (183). Given the importance of the Hedgehog pathway in patterning the midline (174, 175), it is intriguing that *SMARCB1*-mutant meningiomas were primarily found to occur along the midline of both the convexity and anterior skull base. In fact, *GLI1* expression levels in *SMARCB1*-mutant meningiomas more closely resemble *GLI1* levels found in the *SMO*-mutant meningiomas that form along the olfactory groove in the anterior skull base (101). We hypothesize that deregulation of the Hedgehog pathway results in the predilection of these meningiomas to occur along the midline. Further, these results

are consistent with a previous study that demonstrated that germline *SMARCB1* mutations were associated with the development of parafalcine meningiomas (99).

Increased EZH2 Expression and High-Grade Predilection

We found that a considerable percentage (36%) of *SMARCB1*-mutant meningiomas were identified as *de novo* high-grade – this is a greater percentage than is often reported in the literature (5-7). Interestingly, whole-genome genotyping analysis demonstrated that these high-grade *SMARCB1*-mutant lesions possessed remarkable chromosomal stability compared to non-*SMARCB1*-mutant *NF2*-mutant high-grade lesions analyzed in our cohort. While chromosomal instability is typically considered a hallmark of high-grade lesions across many tumor types, these *SMARCB1*-mutant meningiomas appear to progress to high-grade lesions via some other mechanism (187). These data are consistent with previous work that demonstrated that highly malignant rhabdoid tumors that result from *SMARCB1* mutations demonstrate remarkably stable genomes, harboring relatively few genetic point mutations or chromosomal alterations, especially for such an aggressive tumor type (165). One mechanism by which these *SMARCB1*-mutant tumors may progress to high-grade lesions without widespread genomic mutations or chromosomal instability is via epigenetic modifications – either via gene methylation or histone modification. SMARCB1 and the SWI/SNF complex are capable of remodeling chromatin via ATP-dependent nucleosome modulation (119-

121). Interestingly, we also found that *SMARCB1*-mutant meningiomas possessed increased *EZH2* expression compared to both normal meningeal control tissue and non-*SMARCB1*-mutant *NF2*-mutant meningiomas. EZH2 is a member of the Polycomb-group proteins that is capable of epigenetically silencing the expression of a gene via histone methylation, resulting in chromatin remodeling (188-190). Previous studies have indeed demonstrated that the SWI/SNF complex, and the SMARCB1 component specifically, interacts with EZH2 and other Polycomb-group proteins (191-194). These epigenetic modifications, either directly resulting from aberrant function of the SWI/SNF complex or via deregulation of EZH2 expression, may allow affected cells to regress to a more de-differentiated state and progress to high-grade lesions even in the absence of widespread genomic instability.

Taken together, these results demonstrate that *SMARCB1*-mutant meningiomas represent a genetically and phenotypically distinct sub-group of *NF2*-mutant meningiomas and partially contribute to the observed clinical heterogeneity of convexity lesions.

Treatment Implications and Future Directions

The ultimate goal of these genetic analyses is to help identify potential therapeutic targets and enhance our capacity to detect meningiomas with an increased propensity to recur following surgical treatment or progress to high-grade lesions.

These results suggest potential targets for therapeutic intervention and help lay the foundation for future studies to determine if individualized therapies may be efficacious for patients with *SMARCB1*-mutant meningiomas.

The first targetable option that may warrant future exploration would be the Hedgehog pathway. Our results demonstrated that *SMARCB1*-mutant meningiomas demonstrate increased *GLI1* expression and possible deregulation of the Hedgehog pathway that may account for the predilection of these tumors to occur along the midline. Midline tumors of both the convexity and skull base can be difficult to safely cure surgically due to encasement or involvement of critical vessels and structures including the superior sagittal sinus and pericallosal arteries. In these cases, adjuvant chemotherapeutic options may prove helpful in tumor treatment. Many Hedgehog pathway inhibitors exist and are being used in FDA-approved clinical trials (data from https://clinicaltrials.gov/). Future studies are needed to determine if such an inhibitor may be capable of inhibiting tumor growth, recurrence, or progression in *SMARCB1*-mutant meningiomas.

A second potential therapeutic target is EZH2. We have demonstrated that *SMARCB1*-mutant meningiomas trend to having a predilection of being high-grade at time of initial surgery. High-grade meningiomas have significantly increased recurrence rates and significantly more grave prognoses (5, 11-13). One factor contributing to the poor prognosis carried by the high-grade meningiomas is the lack of effective chemotherapeutic therapies to supplement surgical intervention

(14). Here, we found that *SMARCB1*-mutant meningiomas have increased EZH2 levels. Increased EZH2 expression may serve as a substitute for widespread genomic instability and contribute to the progression of these tumors to high-grade lesions (187). Therefore, EZH2 inhibitors may be an efficacious chemotherapeutic option for patients found to have a high-grade *SMARCB1*-mutant meningioma. As was true for the Hedgehog pathway inhibitors, numerous EZH2 inhibitors already exist and are being used in FDA-approved clinical trials (data from https://clinicaltrials.gov/). Again, future studies are needed to determine if such an inhibitor may be capable of inhibiting tumor growth, recurrence, or progression in *SMARCB1*-mutant meningiomas.

An additional area of future study may be the potential role of radiation therapy for patients with high-grade *SMARCB1*-mutant meningiomas. Radiation therapy has been used as an adjuvant to surgical resection of meningiomas; however, its use remains controversial (9, 10, 12, 23). One of the primary concerns is that radiation therapy may induce further genomic instability and contribute to malignant progression of these tumors. In other words, in high-grade tumors that already possess numerous point mutations and widespread chromosomal instability yet are able continue to proliferate, inducing additional point mutations and chromosomal aberrations via radiation therapy may only serve to contribute to malignant progression. However, we found that high-grade meningiomas that harbor *SMARCB1* mutations possess remarkably stable genomes with relatively few point mutations or large-scale chromosomal aberrations. Therefore, it is possible that

these tumors may be amenable to radiation therapy with relatively little risk of significant malignant progression.

In addition to these clinical areas of future study, further work is needed to better understand the role and elucidate the precise mechanisms by which *SMARCB1* mutations contribute to meningioma formation. Further, additional work is needed to identify other concurrently mutated genes and/or epigenetic modifications that account for the observed clinical heterogeneity of other *NF2*-mutant meningiomas.

Conclusion

In summary, we identified somatic *SMARCB1* mutations in a subset of concurrently *NF2*-mutant intracranial meningiomas. These *SMARCB1*-mutant meningiomas represent a distinct genetic and phenotypic sub-group of *NF2*-mutant meningiomas. These tumors primarily occur along the midline – possibly due to aberrant hedgehog signaling and increased *GLI1* expression – and have an increased propensity to be *de novo* high-grade lesions despite having remarkably stable genomes – possibly due to epigenetic alterations due to increased *EZH2* expression. These results help to account for some of the observed clinical heterogeneity of *NF2*-mutant meningiomas. Further, these findings suggest potential targets for therapeutic interventions that warrant future investigation.

APPENDIX

Table A1. Whole-Genome Genotyping Results for Non-*SMARCB1*-Mutant *NF2*-Mutant High-Grade Meningiomas

Tumor Sample	*NF2* Status	*SMARCB1* Status	Tumor Grade	Large-Scale Chr Deletion Events	Focal Chr Deletion Events	Large-Scale Chr Amp. Events	Focal Chr Amp. Events	Large-Scale Chr LOH Events	Focal Chr LOH Events
BONN-T-1134	NF2-mutant / Chr22-loss	Wildtype	2	22q	None	None	None	None	None
BONN-T-1766	NF2-mutant / Chr22-loss	Wildtype	2	19q	19p	None	None	19p / 22q	None
BONN-T-2492	NF2-mutant / Chr22-loss	Wildtype	2	19p / 22q	None	None	None	None	16p
BONN-T-2857	NF2-mutant / Chr22-loss	Wildtype	2	7p / 22q	None	7q	None	None	5p / 16p
BONN-T-2936	NF2-mutant / Chr22-loss	Wildtype	2	1p / 9p / 12p / 19p / 22q	None	None	None	None	None
BONN-T-2983	NF2-mutant / Chr22-loss	Wildtype	2	14q / 22q	16p	None	None	None	None
BONN-T-3811	NF2-mutant / Chr22-loss	Wildtype	2	1p / 8p / 8q / 14q / 22q	None	None	None	None	None
BONN-T-4243	NF2-mutant / Chr22-loss	Wildtype	2	1p / 4p / 4q / 6q / 18p / 18q / 22q	None	7p	None	None	None
BONN-T-4526	NF2-mutant / Chr22-loss	Wildtype	2	None	1p / 2p / 2q / 3p / 3q / 4p / 4q / 5p / 5q / 6p / 6q / 7p / 7q / 8p / 8q / 10p / 10q / 11p / 11q / 12p / 12q / 13q / 14q / 16p / 18p / 18q / 21q / 22q	None	16p	22q	20p
BONN-T-4530	NF2-mutant / Chr22-loss	Wildtype	2	1p / 1q / 4p / 4q / 6p / 6q / 14q / 22q	None	20p / 20q	None	None	16p
BONN-T-4560	NF2-mutant / Chr22-loss	Wildtype	2	22q	None	14q	None	None	14q
BONN-T-4705	NF2-mutant / Chr22-loss	Wildtype	2	1p / 6p / 6q / 14q / 22q	None	None	None	None	None
BONN-T-4760	NF2-mutant / Chr22-loss	Wildtype	2	1p / 6q / 14q / 17p / 18p / 18q / 22q	13q	1q / 13q	17q	None	16p

BONN-T-4846	NF2-mutant / Chr22-loss	Wildtype	2	22q	None	None	None	7p	7q / 14q
BONN-T-590	NF2-mutant / Chr22-loss	Wildtype	2	14q / 22q	None	None	None	11p / 19q	None
BONN-T-83	NF2-mutant / Chr22-loss	Wildtype	2	1p / 7p / 9p / 10p / 10q / 14q / 18q / 22q	None	1q	3q	None	None
MUN-MN-164	NF2-mutant / Chr22-loss	Wildtype	2	1p / 2p / 7p / 7q / 18p / 18q / 22q	None	3p / 3q / 5p / 5q / 8p / 8q / 9p / 20p	9q	6p / 6q / 15q / 16p / 16q / 20q / 21q	9q / 20p
MUN-MN-171	NF2-mutant / Chr22-loss	Wildtype	2	1p / 10p / 10q / 14q / 18p / 18q / 22q	None	13q	1q	None	None
MUN-MN-22	NF2-mutant / Chr22-loss	Wildtype	2	22q	None	None	None	None	16p
MUN-MN-298	NF2-mutant / Chr22-loss	Wildtype	2	1p / 12p / 22q	None	None	None	None	None
MUN-MN-54	NF2-mutant / Chr22-loss	Wildtype	2	1p / 18q / 19p / 22q	None	None	None	None	None
MUN-MN-96	NF2-mutant / Chr22-loss	Wildtype	2	1p / 6p / 6q / 10q / 12q / 14q / 19p / 22q	10p	10p	9q	8p	8q / 10p / 10q / 14q / 19p
MUN-MN-97	NF2-mutant / Chr22-loss	Wildtype	2	1p / 6p / 6q / 7p / 10p / 10q / 14q / 22q	None	None	None	2p / 11p	10q / 19p
YALE-54	NF2-mutant / Chr22-loss	Wildtype	2	1p / 2q / 3p / 6q / 22q	4q	None	None	None	None
YALE-67	NF2-mutant / Chr22-loss	Wildtype	2	1p / 3p / 8p / 8q / 9p / 19p / 22q	None	None	None	None	None
YALE-83	NF2-mutant / Chr22-loss	Wildtype	2	1p / 6q / 11p / 14q / 22q	None	1q / 20p / 20q	None	None	17q

Chr = Chromosomal

Amp. = Amplification

LOH = Loss of Heterozygosity

Table A2. Top 300 Differentially Expressed Genes Between *SMARCB1*-Mutant and Non-*SMARCB1*-Mutant *NF2*-Mutant Meningiomas

Gene	Mean *SMARCB1*-Mutant Meningioma Expression	Mean Non-*SMARCB1*-Mutant *NF2*-Mutant Meningioma Expression	Difference Between *SMARCB1*-Mutant and Non-*SMARCB1*-Mutant *NF2*-Mutant Meningioma
SCG2	10.529	8.097	2.432
RSPO3	9.684	7.328	2.356
FNDC1	7.521	5.306	2.215
NNMT	9.137	7.206	1.931
FBLN1	11.381	9.481	1.900
SFRP1	10.779	8.913	1.866
TNC	8.652	6.805	1.847
SRPX	8.870	7.193	1.677
RBP4	7.043	5.439	1.604
FAM164C	9.959	8.388	1.571
HP	6.723	5.160	1.562
C13orf36	7.041	5.534	1.507
RUNX3	7.927	6.426	1.502
IGF1	7.575	6.097	1.478
COL8A1	11.650	10.248	1.402
VIT	6.726	5.396	1.330
ODZ3	10.326	9.023	1.303
ALPL	10.152	8.851	1.301
CD177	6.229	4.970	1.259
SLPI	11.029	9.781	1.248
MATN2	10.263	9.045	1.217
EGFL6	11.910	10.703	1.207
CHN2	8.465	7.272	1.193
ROR1	8.183	6.997	1.186
HOXC8	6.543	5.358	1.185
C21orf81	8.323	7.150	1.174
RYR3	5.963	4.803	1.160
GFRA1	8.182	7.030	1.152
GDF10	6.945	5.798	1.147
MRAP2	7.923	6.777	1.145
CR622072	9.250	8.107	1.143
TNNC1	10.882	9.746	1.136
NXPH2	8.746	7.621	1.125

Gene	Mean *SMARCB1*-Mutant Meningioma Expression	Mean Non-*SMARCB1*-Mutant *NF2*-Mutant Meningioma Expression	Difference Between *SMARCB1*-Mutant and Non-*SMARCB1*-Mutant *NF2*-Mutant Meningioma
KRT18	7.634	9.683	-2.049
FLJ40504	6.623	8.643	-2.020
NDUFA4L2	8.063	9.923	-1.860
PFKP	6.191	7.872	-1.681
IGFBP3	7.323	8.869	-1.546
LUM	5.707	7.205	-1.497
C4orf31	6.947	8.421	-1.474
EFNB2	7.223	8.688	-1.465
IGF2	6.786	8.249	-1.463
HOPX	6.997	8.457	-1.460
SCG5	5.349	6.779	-1.430
PVALB	4.745	6.164	-1.420
DAPL1	4.940	6.341	-1.401
PERP	6.202	7.593	-1.391
DIRAS2	5.603	6.978	-1.376
DCN	6.429	7.795	-1.366
SEZ6L2	7.444	8.806	-1.362
SYBU	7.947	9.295	-1.348
VTN	6.175	7.510	-1.335
PHLDA1	5.691	7.010	-1.319
TF	6.286	7.602	-1.316
CDKN2C	6.370	7.667	-1.297
NECAB1	7.713	8.996	-1.283
AGR2	4.696	5.971	-1.276
GJB6	6.801	8.076	-1.275
LINGO2	5.058	6.302	-1.244
NPNT	7.402	8.642	-1.240
APOD	8.179	9.419	-1.240
RPS4Y1	5.784	7.015	-1.230
ANGPT2	5.647	6.867	-1.220
CAMK2N1	7.052	8.226	-1.174
STC2	5.102	6.267	-1.165
H19	8.390	9.543	-1.152

ZBTB7C	8.409	7.285	1.124	*APOLD1*	7.097	8.228	-1.131
COL8A2	9.843	8.728	1.115	*ATP1A2*	4.865	5.985	-1.121
BCAR3	8.242	7.132	1.109	*PDGFRA*	4.861	5.957	-1.096
PRRX1	10.647	9.539	1.108	*CA3*	5.815	6.906	-1.091
HOXC9	5.911	4.815	1.095	*NEBL*	6.045	7.130	-1.085
NTN1	8.801	7.717	1.085	*PDLIM1*	6.443	7.527	-1.084
MYOZ3	8.369	7.292	1.077	*CFI*	7.528	8.585	-1.057
KIAA1644	6.722	5.649	1.073	*C1QTNF1*	7.958	9.010	-1.052
ACAN	5.846	4.777	1.069	*PDE5A*	7.877	8.919	-1.042
CNTN3	6.580	5.513	1.067	*RELN*	4.535	5.569	-1.034
XIST	8.396	7.328	1.067	*BMP6*	6.412	7.444	-1.033
TGFB3	9.006	7.960	1.046	*PDE7B*	5.853	6.884	-1.031
SLC35F2	7.317	6.274	1.043	*RNASE1*	8.029	9.056	-1.027
PODXL2	7.460	6.424	1.036	*PAPLN*	6.442	7.457	-1.015
DUOX1	6.610	5.577	1.033	*FREM2*	4.684	5.694	-1.010
SMAD9	8.198	7.177	1.021	*CXCL12*	6.785	7.791	-1.006
NDRG4	6.885	5.864	1.021	*MET*	6.739	7.741	-1.002
FABP5	10.854	9.834	1.021	*SLC26A2*	7.702	8.702	-1.000
SORCS2	6.937	5.917	1.020	*FOLR2*	6.689	7.688	-0.999
DLL1	7.289	6.273	1.016	*KCNT2*	5.592	6.587	-0.995
NT5DC2	8.711	7.696	1.015	*EIF1AY*	4.755	5.745	-0.990
CDH23	9.482	8.488	0.994	*HEY1*	6.179	7.169	-0.989
FAM180B	7.407	6.414	0.993	*SLC7A2*	9.660	10.639	-0.979
KLK7	5.946	4.958	0.988	*KCNJ8*	7.180	8.157	-0.977
MFAP5	11.482	10.497	0.985	*RHOJ*	5.507	6.472	-0.965
FAM132A	6.384	5.400	0.984	*PTGDS*	11.527	12.479	-0.952
PXDN	8.773	7.797	0.977	*GJA3*	4.432	5.383	-0.951
IL20RA	5.799	4.825	0.974	*SIPA1L2*	6.469	7.415	-0.946
FAM107B	9.295	8.323	0.972	*PPP1R1B*	5.078	6.023	-0.945
SLC6A4	5.603	4.632	0.971	*GAP43*	6.238	7.181	-0.943
ISM1	7.262	6.290	0.971	*AHNAK2*	7.291	8.232	-0.941
TRIM9	5.922	4.960	0.962	*NR3C2*	6.042	6.982	-0.940
ROBO3	8.044	7.082	0.962	*SNAR-A3*	5.676	6.614	-0.938
PRPH	6.506	5.545	0.962	*COL18A1*	6.042	6.973	-0.932
HPR	6.905	5.948	0.957	*DCLK1*	5.930	6.862	-0.932
HAPLN3	5.977	5.035	0.942	*RAPGEF5*	5.823	6.748	-0.925
MT1E	9.808	8.866	0.942	*APCDD1*	5.876	6.796	-0.920
MFGE8	11.758	10.819	0.938	*AGT*	4.969	5.884	-0.915
CTXN3	9.070	8.134	0.935	*STRA6*	4.574	5.483	-0.908
TMEM158	9.150	8.219	0.932	*PDE8B*	6.546	7.451	-0.905
TSPAN11	5.934	5.003	0.931	*RAB27B*	4.366	5.255	-0.888

COL23A1	6.023	5.092	0.931	*PLTP*	5.992	6.865	-0.873
TOX2	7.703	6.777	0.925	*MAPK4*	4.984	5.856	-0.872
MYLK	8.037	7.116	0.922	*WDR86*	8.249	9.103	-0.855
HEG1	9.178	8.259	0.919	*FAM179A*	5.094	5.946	-0.852
SLCO3A1	7.575	6.664	0.911	*TPM2*	10.467	11.319	-0.852
NELL1	6.218	5.307	0.911	*ACTG2*	6.129	6.980	-0.851
SNAP91	7.530	6.619	0.911	*HSD17B2*	5.652	6.502	-0.849
DLGAP2	5.934	5.025	0.909	*PRKAG2*	7.137	7.982	-0.845
RNF144A	6.818	5.916	0.903	*TFPI*	5.009	5.850	-0.841
ATP1B1	10.519	9.617	0.902	*KCNK1*	4.842	5.680	-0.837
ST8SIA1	6.750	5.852	0.897	*EDN3*	4.479	5.312	-0.833
IL17RB	6.271	5.379	0.892	*F3*	7.292	8.124	-0.833
CLIC3	9.721	8.830	0.891	*TNFRSF11B*	7.284	8.116	-0.832
ODZ4	8.323	7.438	0.885	*C21orf62*	4.832	5.662	-0.830
FAM180A	5.783	4.900	0.883	*ALDH1A3*	4.668	5.493	-0.825
NKD1	6.327	5.447	0.880	*ELOVL2*	4.883	5.708	-0.825
MYRIP	5.632	4.755	0.877	*NLGN1*	5.633	6.456	-0.824
EFHD1	8.324	7.448	0.877	*ABCB1*	5.104	5.927	-0.823
PPAP2B	10.320	9.444	0.876	*ACHE*	4.959	5.782	-0.823
FAM69C	5.325	4.458	0.867	*RNFT2*	6.105	6.916	-0.811
FZD9	6.740	5.877	0.863	*OLFML2B*	8.281	9.088	-0.807
NRXN2	8.370	7.509	0.862	*F10*	6.067	6.866	-0.799
MT1M	6.970	6.115	0.855	*ADAMTS1*	5.159	5.954	-0.795
C2orf55	9.063	8.209	0.853	*LRRC17*	6.265	7.059	-0.794
CDH5	9.514	8.664	0.851	*LOC644936*	7.648	8.441	-0.793
SLC39A14	8.436	7.588	0.847	*ATP6V1G2*	5.588	6.379	-0.791
NAV2	8.137	7.291	0.845	*POSTN*	4.678	5.451	-0.773
SHROOM3	7.056	6.211	0.845	*AF385432*	5.400	6.172	-0.772
MAMSTR	6.952	6.111	0.842	*ISYNA1*	7.554	8.320	-0.766
GLI1	6.169	5.329	0.840	*BAMBI*	8.746	9.512	-0.766
SHF	7.372	6.539	0.832	*GAS2*	4.625	5.389	-0.764
SERPINF1	9.646	8.815	0.831	*S100A13*	5.282	6.041	-0.759
KIF1A	8.525	7.696	0.830	*SEMA3C*	6.586	7.344	-0.759
SHC4	7.782	6.952	0.830	*REEP2*	4.714	5.472	-0.758
ST6GAL1	10.971	10.145	0.826	*LAYN*	6.493	7.245	-0.752
ANKRD20A4	8.176	7.356	0.820	*F13A1*	6.537	7.288	-0.751
SFRP4	10.262	9.445	0.817	*LOC100131176*	5.000	5.750	-0.750
RNF24	7.276	6.461	0.815	*HYAL1*	6.444	7.193	-0.749
SCARA5	12.305	11.494	0.811	*IGSF5*	4.622	5.370	-0.749
JAK2	7.553	6.745	0.808	*PALMD*	5.708	6.455	-0.747
SPON1	7.072	6.266	0.806	*IL8*	5.241	5.986	-0.745

REEP1	9.131	8.331	0.800	*CA8*	5.002	5.744	-0.742
MXRA8	8.542	7.746	0.796	*FAM134B*	7.214	7.955	-0.741
CGNL1	11.176	10.382	0.794	*LYVE1*	6.592	7.332	-0.740
ATOH8	8.516	7.727	0.789	*RCN1*	9.905	10.640	-0.735
B4GALT1	8.155	7.369	0.786	*TNFRSF12A*	5.920	6.653	-0.733
MT1X	10.102	9.316	0.786	*CFH*	7.439	8.172	-0.733
NEUROG2	6.399	5.617	0.782	*RCAN2*	6.184	6.915	-0.731
CALML4	9.113	8.332	0.782	*PANK1*	6.330	7.060	-0.730
FGL2	12.483	11.713	0.771	*FAM129A*	7.549	8.271	-0.722
BOC	8.818	8.048	0.770	*TMEM108*	6.529	7.251	-0.722
CSRP2	8.466	7.702	0.765	*BMP5*	8.093	8.814	-0.721
PRDM6	7.471	6.708	0.763	*GCNT2*	5.470	6.189	-0.719
BBS9	7.617	6.855	0.761	*C5orf30*	5.612	6.329	-0.718
RAP1GAP	6.849	6.089	0.760	*FLJ30375*	6.322	7.039	-0.718
NEDD4L	7.284	6.527	0.757	*S100A9*	5.728	6.445	-0.717
IL11RA	10.930	10.176	0.754	*HEY2*	5.378	6.095	-0.717
RAB31	11.203	10.453	0.751	*WFDC2*	5.001	5.717	-0.716
ITGA11	7.642	6.892	0.750	*CPS1*	6.297	7.011	-0.714
AR	7.110	6.362	0.748	*ISLR*	9.903	10.616	-0.713
LDLRAD3	5.962	5.214	0.747	*CXXC5*	8.344	9.056	-0.712
MAP1B	10.193	9.447	0.746	*PDE6A*	5.397	6.107	-0.710
THBS4	5.857	5.111	0.746	*SERPINA3*	6.623	7.329	-0.706
CPT1C	6.660	5.914	0.746	*CAV2*	6.003	6.707	-0.704
C1QTNF4	5.992	5.247	0.745	*ENPP5*	6.048	6.750	-0.702
PIK3R1	10.581	9.841	0.740	*LTBP4*	9.234	9.935	-0.702
FAM38B	8.165	7.427	0.738	*GPR83*	6.750	7.450	-0.700
CYP4B1	6.622	5.888	0.734	*CCND1*	11.669	12.368	-0.699
ARHGEF3	10.048	9.317	0.731	*ABCC9*	5.391	6.089	-0.698
SLC38A8	5.515	4.785	0.730	*ANGPT1*	5.620	6.318	-0.698
RCN3	7.928	7.198	0.730	*DHRS2*	4.472	5.169	-0.697
CAB39L	8.592	7.863	0.729	*TAGLN2*	8.675	9.372	-0.697
TMEM59L	6.720	5.992	0.728	*NXPH4*	4.807	5.503	-0.696
EFS	8.138	7.410	0.728	*SYTL4*	4.966	5.661	-0.695
RUNX1	7.482	6.757	0.725	*ALDH1A2*	6.278	6.969	-0.691
CYP1B1	11.347	10.624	0.723	*IGDCC4*	5.464	6.155	-0.691

Table A3. Comparison of Demographic Data Between *SMARCB1*-Mutant and Non-*SMARCB1*-Mutant *NF2*-Mutant High-Grade Meningiomas

Tumor Sample	*SMARCB1* Status	*NF2* Status	Tumor Grade	Patient Age (years)	Patient Gender
BONN-T-1134	Wildtype	*NF2*-mutant / Chr22-loss	2	44	F
BONN-T-1766	Wildtype	*NF2*-mutant / Chr22-loss	2	70	M
BONN-T-2492	Wildtype	*NF2*-mutant / Chr22-loss	2	56	F
BONN-T-2857	Wildtype	*NF2*-mutant / Chr22-loss	2	53	M
BONN-T-2936	Wildtype	*NF2*-mutant / Chr22-loss	2	66	F
BONN-T-2983	Wildtype	*NF2*-mutant / Chr22-loss	2	76	M
BONN-T-3811	Wildtype	*NF2*-mutant / Chr22-loss	2	68	M
BONN-T-4243	Wildtype	*NF2*-mutant / Chr22-loss	2	86	M
BONN-T-4526	Wildtype	*NF2*-mutant / Chr22-loss	2	64	F
BONN-T-4530	Wildtype	*NF2*-mutant / Chr22-loss	2	54	M
BONN-T-4560	Wildtype	*NF2*-mutant / Chr22-loss	2	77	F
BONN-T-4705	Wildtype	*NF2*-mutant / Chr22-loss	2	94	M
BONN-T-4760	Wildtype	*NF2*-mutant / Chr22-loss	2	86	M
BONN-T-4846	Wildtype	*NF2*-mutant / Chr22-loss	2	78	F
BONN-T-590	Wildtype	*NF2*-mutant / Chr22-loss	2	63	F
BONN-T-83	Wildtype	*NF2*-mutant / Chr22-loss	2	56	M
MUN-MN-164	Wildtype	*NF2*-mutant / Chr22-loss	2	45	F
MUN-MN-171	Wildtype	*NF2*-mutant / Chr22-loss	2	53	F
MUN-MN-22	Wildtype	*NF2*-mutant / Chr22-loss	2	50	F
MUN-MN-298	Wildtype	*NF2*-mutant / Chr22-loss	2	23	F
MUN-MN-54	Wildtype	*NF2*-mutant / Chr22-loss	2	56	M
MUN-MN-96	Wildtype	*NF2*-mutant / Chr22-loss	2	76	M
MUN-MN-97	Wildtype	*NF2*-mutant / Chr22-loss	2	59	M
YALE-54	Wildtype	*NF2*-mutant / Chr22-loss	2	62	F
YALE-67	Wildtype	*NF2*-mutant / Chr22-loss	2	39	F
YALE-83	Wildtype	*NF2*-mutant / Chr22-loss	2	n/a	F

Tumor Sample	*SMARCB1* Mutation	*NF2* Status	Tumor Grade	Patient Age (years)	Patient Gender
BONN-T-2758	R386H	*NF2*-mutant	2	65	M
BONN-T-314	R383Q	Chr22q-loss & *NF2*-mutant	2	49	F
BONN-T-439	R386H	*NF2*-mutant	2	72	M
BONN-T-841	R386H	Chr22q-loss	2	67	M
BONN-T-847	Frameshift	*NF2*-mutant	2	59	F
KOLN-HT-2835	Frameshift	*NF2*-mutant	2	73	M
MSK-MN-500	R386H	*NF2*-loss & *NF2*-mutant	2	64	F
MUN-MN-295	Frameshift	Chr22q-loss	2	70	F
YALE-251	R386H	*NF2*-loss	2	29	F

	Non-*SMARCB1*-Mutant	*SMARCB1*-Mutant
Median Age	62	65
% Female	54%	55%

REFERENCES

1. Dolecek T. A., Propp J. M., Stroup N. E., and Kruchko C. CBTRUS statistical report: primary brain and central nervous system tumors diagnosed in the United States in 2005-2009. *Neuro Oncol.* 2012;14 Suppl 5(v1-49.

2. Louis D. N., Ohgaki H., Wiestler O. D., Cavenee W. K., Burger P. C., et al. The 2007 WHO classification of tumours of the central nervous system. *Acta Neuropathol.* 2007;114(2):97-109.

3. Claus E. B., Bondy M. L., Schildkraut J. M., Wiemels J. L., Wrensch M., et al. Epidemiology of intracranial meningioma. *Neurosurgery.* 2005;57(6):1088-95; discussion -95.

4. Whittle I. R., Smith C., Navoo P., and Collie D. Meningiomas. *Lancet.* 2004;363(9420):1535-43.

5. Riemenschneider M. J., Perry A., and Reifenberger G. Histological classification and molecular genetics of meningiomas. *Lancet Neurol.* 2006;5(12):1045-54.

6. Willis J., Smith C., Ironside J. W., Erridge S., Whittle I. R., et al. The accuracy of meningioma grading: a 10-year retrospective audit. *Neuropathol Appl Neurobiol.* 2005;31(2):141-9.

7. Perry A., Scheithauer B. W., Stafford S. L., Lohse C. M., and Wollan P. C. "Malignancy" in meningiomas: a clinicopathologic study of 116 patients, with grading implications. *Cancer.* 1999;85(9):2046-56.

8. Fathi A. R., and Roelcke U. Meningioma. *Curr Neurol Neurosci Rep.* 2013;13(4):337.

9. Marosi C., Hassler M., Roessler K., Reni M., Sant M., et al. Meningioma. *Crit Rev Oncol Hematol.* 2008;67(2):153-71.

10. van Alkemade H., de Leau M., Dieleman E. M., Kardaun J. W., van Os R., et al. Impaired survival and long-term neurological problems in benign meningioma. *Neuro Oncol.* 2012;14(5):658-66.

11. Durand A., Labrousse F., Jouvet A., Bauchet L., Kalamarides M., et al. WHO grade II and III meningiomas: a study of prognostic factors. *J Neurooncol.* 2009;95(3):367-75.

12. Choy W., Kim W., Nagasawa D., Stramotas S., Yew A., et al. The molecular genetics and tumor pathogenesis of meningiomas and the future directions of meningioma treatments. *Neurosurg Focus.* 2011;30(5):E6.

13. Palma L., Celli P., Franco C., Cervoni L., and Cantore G. Long-term prognosis for atypical and malignant meningiomas: a study of 71 surgical cases. *J Neurosurg.* 1997;86(5):793-800.

14. Wen P. Y., Quant E., Drappatz J., Beroukhim R., and Norden A. D. Medical therapies for meningiomas. *J Neurooncol.* 2010;99(3):365-78.

15. Goutagny S., Yang H. W., Zucman-Rossi J., Chan J., Dreyfuss J. M., et al. Genomic profiling reveals alternative genetic pathways of meningioma malignant progression dependent on the underlying NF2 status. *Clin Cancer Res.* 2010;16(16):4155-64.

16. Krayenbuhl N., Pravdenkova S., and Al-Mefty O. De novo versus transformed atypical and anaplastic meningiomas: comparisons of clinical course, cytogenetics, cytokinetics, and outcome. *Neurosurgery.* 2007;61(3):495-503; discussion -4.

17. Greenberg M. S., and Greenberg M. S. *Handbook of neurosurgery.* Tampa, Fla.: Greenberg Graphics ;; 2010.

18. Wang D. J., Xie Q., Gong Y., Mao Y., Wang Y., et al. Histopathological classification and location of consecutively operated meningiomas at a single institution in China from 2001 to 2010. *Chin Med J (Engl).* 2013;126(3):488-93.

19. Kane A. J., Sughrue M. E., Rutkowski M. J., Shangari G., Fang S., et al. Anatomic location is a risk factor for atypical and malignant meningiomas. *Cancer.* 2011;117(6):1272-8.

20. McGovern S. L., Aldape K. D., Munsell M. F., Mahajan A., DeMonte F., et al. A comparison of World Health Organization tumor grades at recurrence in patients with non-skull base and skull base meningiomas. *J Neurosurg.* 2010;112(5):925-33.

21. Sade B., Chahlavi A., Krishnaney A., Nagel S., Choi E., et al. World Health Organization Grades II and III meningiomas are rare in the cranial base and spine. *Neurosurgery.* 2007;61(6):1194-8; discussion 8.

22. Wiemels J., Wrensch M., and Claus E. B. Epidemiology and etiology of meningioma. *J Neurooncol.* 2010;99(3):307-14.

23. Gondi V., Tome W. A., and Mehta M. P. Fractionated radiotherapy for intracranial meningiomas. *J Neurooncol.* 2010;99(3):349-56.

24. Mardis E. R. The impact of next-generation sequencing technology on genetics. *Trends Genet.* 2008;24(3):133-41.

25. Shendure J., and Ji H. Next-generation DNA sequencing. *Nat Biotechnol.* 2008;26(10):1135-45.

26. Bilguvar K., Ozturk A. K., Louvi A., Kwan K. Y., Choi M., et al. Whole-exome sequencing identifies recessive WDR62 mutations in severe brain malformations. *Nature.* 2010;467(7312):207-10.

27. Mardis E. R., and Wilson R. K. Cancer genome sequencing: a review. *Hum Mol Genet.* 2009;18(R2):R163-8.

28. Bamshad M. J., Ng S. B., Bigham A. W., Tabor H. K., Emond M. J., et al. Exome sequencing as a tool for Mendelian disease gene discovery. *Nat Rev Genet.* 2011;12(11):745-55.

29. Mishra-Gorur K., Caglayan A. O., Schaffer A. E., Chabu C., Henegariu O., et al. Mutations in KATNB1 Cause Complex Cerebral Malformations by Disrupting Asymmetrically Dividing Neural Progenitors. *Neuron.* 2014;84(6):1226-39.

30. Novarino G., Fenstermaker A. G., Zaki M. S., Hofree M., Silhavy J. L., et al. Exome sequencing links corticospinal motor neuron disease to common neurodegenerative disorders. *Science.* 2014;343(6170):506-11.

31. Schaffer A. E., Eggens V. R., Caglayan A. O., Reuter M. S., Scott E., et al. CLP1 founder mutation links tRNA splicing and maturation to cerebellar development and neurodegeneration. *Cell.* 2014;157(3):651-63.

32. Bea S., Valdes-Mas R., Navarro A., Salaverria I., Martin-Garcia D., et al. Landscape of somatic mutations and clonal evolution in mantle cell lymphoma. *Proc Natl Acad Sci U S A.* 2013;110(45):18250-5.

33. Cooke S. L., Marshall J., Martincorena I., Hinton J., Gundem G., et al. Recurrent mutations in epigenetic regulators, RHOA and FYN kinase in peripheral T cell lymphomas. *Nat Genet.* 2014;46(2):166-70.

34. Holmfeldt L., Wei L., Diaz-Flores E., Walsh M., Zhang J., et al. The genomic landscape of hypodiploid acute lymphoblastic leukemia. *Nat Genet.* 2013;45(3):242-52.

35. Lohr J. G., Stojanov P., Lawrence M. S., Auclair D., Chapuy B., et al. Discovery and prioritization of somatic mutations in diffuse large B-cell lymphoma (DLBCL) by whole-exome sequencing. *Proc Natl Acad Sci U S A.* 2012;109(10):3879-84.

36. Okosun J., Bodor C., Wang J., Araf S., Yang C. Y., et al. Integrated genomic analysis identifies recurrent mutations and evolution patterns driving the initiation and progression of follicular lymphoma. *Nat Genet.* 2014;46(2):176-81.

37. Papaemmanuil E., Rapado I., Li Y., Potter N. E., Wedge D. C., et al. RAG-mediated recombination is the predominant driver of oncogenic rearrangement in ETV6-RUNX1 acute lymphoblastic leukemia. 2014;46(2):116-25.

38. Quesada V., Conde L., Villamor N., Ordonez G. R., Jares P., et al. Exome sequencing identifies recurrent mutations of the splicing factor SF3B1 gene in chronic lymphocytic leukemia. *Nat Genet.* 2012;44(1):47-52.

39. Richter J., Schlesner M., Hoffmann S., Kreuz M., Leich E., et al. Recurrent mutation of the ID3 gene in Burkitt lymphoma identified by integrated genome, exome and transcriptome sequencing. *Nat Genet.* 2012;44(12):1316-20.

40. Sakaguchi H., Okuno Y., Muramatsu H., Yoshida K., Shiraishi Y., et al. Exome sequencing identifies secondary mutations of SETBP1 and JAK3 in juvenile myelomonocytic leukemia. *Nat Genet.* 2013;45(8):937-41.

41. Tiacci E., Trifonov V., Schiavoni G., Holmes A., Kern W., et al. BRAF mutations in hairy-cell leukemia. *N Engl J Med.* 2011;364(24):2305-15.

42. Wang L., Lawrence M. S., Wan Y., Stojanov P., Sougnez C., et al. SF3B1 and other novel cancer genes in chronic lymphocytic leukemia. *N Engl J Med.* 2011;365(26):2497-506.

43. Gartner J. J., Parker S. C., Prickett T. D., Dutton-Regester K., Stitzel M. L., et al. Whole-genome sequencing identifies a recurrent functional synonymous mutation in melanoma. *Proc Natl Acad Sci U S A.* 2013;110(33):13481-6.

44. Wei X., Walia V., Lin J. C., Teer J. K., Prickett T. D., et al. Exome sequencing identifies GRIN2A as frequently mutated in melanoma. *Nat Genet.* 2011;43(5):442-6.

45. Pena-Llopis S., Vega-Rubin-de-Celis S., Liao A., Leng N., Pavia-Jimenez A., et al. BAP1 loss defines a new class of renal cell carcinoma. *Nat Genet.* 2012;44(7):751-9.

46. Sato Y., Yoshizato T., Shiraishi Y., Maekawa S., Okuno Y., et al. Integrated molecular analysis of clear-cell renal cell carcinoma. *Nat Genet.* 2013;45(8):860-7.

47. Agrawal N., Frederick M. J., Pickering C. R., Bettegowda C., Chang K., et al. Exome sequencing of head and neck squamous cell carcinoma reveals inactivating mutations in NOTCH1. *Science.* 2011;333(6046):1154-7.

48. Lui V. W., Peyser N. D., Ng P. K., Hritz J., Zeng Y., et al. Frequent mutation of receptor protein tyrosine phosphatases provides a mechanism for STAT3

hyperactivation in head and neck cancer. *Proc Natl Acad Sci U S A.* 2014;111(3):1114-9.

49. Stransky N., Egloff A. M., Tward A. D., Kostic A. D., Cibulskis K., et al. The mutational landscape of head and neck squamous cell carcinoma. *Science.* 2011;333(6046):1157-60.

50. Banerji S., Cibulskis K., Rangel-Escareno C., Brown K. K., Carter S. L., et al. Sequence analysis of mutations and translocations across breast cancer subtypes. *Nature.* 2012;486(7403):405-9.

51. Ellis M. J., Ding L., Shen D., Luo J., Suman V. J., et al. Whole-genome analysis informs breast cancer response to aromatase inhibition. *Nature.* 2012;486(7403):353-60.

52. Robinson D. R., Wu Y. M., Vats P., Su F., Lonigro R. J., et al. Activating ESR1 mutations in hormone-resistant metastatic breast cancer. *Nat Genet.* 2013;45(12):1446-51.

53. Wang Y., Waters J., Leung M. L., Unruh A., Roh W., et al. Clonal evolution in breast cancer revealed by single nucleus genome sequencing. *Nature.* 2014;512(7513):155-60.

54. Totoki Y., Tatsuno K., Yamamoto S., Arai Y., Hosoda F., et al. High-resolution characterization of a hepatocellular carcinoma genome. *Nat Genet.* 2011;43(5):464-9.

55. Vilarinho S., Erson-Omay E. Z., Harmanci A. S., Morotti R., Carrion-Grant G., et al. Paediatric hepatocellular carcinoma due to somatic CTNNB1 and NFE2L2 mutations in the setting of inherited bi-allelic ABCB11 mutations. *J Hepatol.* 2014;61(5):1178-83.

56. Imielinski M., Berger A. H., Hammerman P. S., Hernandez B., Pugh T. J., et al. Mapping the hallmarks of lung adenocarcinoma with massively parallel sequencing. *Cell.* 2012;150(6):1107-20.

57. Zhang J., Fujimoto J., Zhang J., Wedge D. C., Song X., et al. Intratumor heterogeneity in localized lung adenocarcinomas delineated by multiregion sequencing. *Science.* 2014;346(6206):256-9.

58. Dulak A. M., Stojanov P., Peng S., Lawrence M. S., Fox C., et al. Exome and whole-genome sequencing of esophageal adenocarcinoma identifies recurrent driver events and mutational complexity. *Nat Genet.* 2013;45(5):478-86.

59. Lin D. C., Hao J. J., Nagata Y., Xu L., Shang L., et al. Genomic and molecular characterization of esophageal squamous cell carcinoma. 2014;46(5):467-73.

60. Nones K., Waddell N., Wayte N., Patch A. M., Bailey P., et al. Genomic catastrophes frequently arise in esophageal adenocarcinoma and drive tumorigenesis. *Nature.* 2014;5(5224.

61. Varela A. M., Ding L. W., Garg M., Liu L. Z., Yang H., et al. Identification of genomic alterations in oesophageal squamous cell cancer. *Nat Genet.* 2014;509(7498):91-5.

62. Wu J., Jiao Y., Dal Molin M., Maitra A., de Wilde R. F., et al. Whole-exome sequencing of neoplastic cysts of the pancreas reveals recurrent mutations in components of ubiquitin-dependent pathways. *Proc Natl Acad Sci U S A.* 2011;108(52):21188-93.

63. Kumar A., White T. A., MacKenzie A. P., Clegg N., Lee C., et al. Exome sequencing identifies a spectrum of mutation frequencies in advanced and lethal prostate cancers. *Proc Natl Acad Sci U S A.* 2011;108(41):17087-92.

64. Jones S., Stransky N., McCord C. L., Cerami E., Lagowski J., et al. Genomic analyses of gynaecologic carcinosarcomas reveal frequent mutations in chromatin remodelling genes. *Nat Commun.* 2014;5(5006.

65. Le Gallo M., O'Hara A. J., Rudd M. L., Urick M. E., Hansen N. F., et al. Exome sequencing of serous endometrial tumors identifies recurrent somatic mutations in chromatin-remodeling and ubiquitin ligase complex genes. *Nat Genet.* 2012;44(12):1310-5.

66. Zhao S., Choi M., Overton J. D., Bellone S., Roque D. M., et al. Landscape of somatic single-nucleotide and copy-number mutations in uterine serous carcinoma. *Proc Natl Acad Sci U S A.* 2013;110(8):2916-21.

67. Mack S. C., Witt H., Piro R. M., Gu L., Zuyderduyn S., et al. Epigenomic alterations define lethal CIMP-positive ependymomas of infancy. *Nature.* 2014;506(7489):445-50.

68. Pugh T. J., Weeraratne S. D., Archer T. C., Pomeranz Krummel D. A., Auclair D., et al. Medulloblastoma exome sequencing uncovers subtype-specific somatic mutations. *Nature.* 2012;488(7409):106-10.

69. Brastianos P. K., Taylor-Weiner A., Manley P. E., Jones R. T., Dias-Santagata D., et al. Exome sequencing identifies BRAF mutations in papillary craniopharyngiomas. *Nat Genet.* 2014;46(2):161-5.

70. Robinson D. R., Wu Y. M., Kalyana-Sundaram S., Cao X., Lonigro R. J., et al. Identification of recurrent NAB2-STAT6 gene fusions in solitary fibrous tumor by integrative sequencing. *Nat Genet.* 2013;45(2):180-5.

71. Fontebasso A. M., Schwartzentruber J., Khuong-Quang D. A., Liu X. Y., Sturm D., et al. Mutations in SETD2 and genes affecting histone H3K36 methylation target hemispheric high-grade gliomas. *Acta Neuropathol.* 2013;125(5):659-69.

72. Wu G., Diaz A. K., Paugh B. S., Rankin S. L., Ju B., et al. The genomic landscape of diffuse intrinsic pontine glioma and pediatric non-brainstem high-grade glioma. *Nat Genet.* 2014;46(5):444-50.

73. Tran E., Turcotte S., Gros A., Robbins P. F., Lu Y. C., et al. Cancer immunotherapy based on mutation-specific CD4+ T cells in a patient with epithelial cancer. *Science.* 2014;344(6184):641-5.

74. Malkin D. Li-fraumeni syndrome. *Genes Cancer.* 2011;2(4):475-84.

75. Spirio L. N., Samowitz W., Robertson J., Robertson M., Burt R. W., et al. Alleles of APC modulate the frequency and classes of mutations that lead to colon polyps. *Nat Genet.* 1998;20(4):385-8.

76. Davies H., Bignell G. R., Cox C., Stephens P., Edkins S., et al. Mutations of the BRAF gene in human cancer. *Nature.* 2002;417(6892):949-54.

77. Rouleau G. A., Merel P., Lutchman M., Sanson M., Zucman J., et al. Alteration in a new gene encoding a putative membrane-organizing protein causes neuro-fibromatosis type 2. *Nature.* 1993;363(6429):515-21.

78. Lallemand D., Curto M., Saotome I., Giovannini M., and McClatchey A. I. NF2 deficiency promotes tumorigenesis and metastasis by destabilizing adherens junctions. *Genes Dev.* 2003;17(9):1090-100.

79. Scoles D. R., Huynh D. P., Morcos P. A., Coulsell E. R., Robinson N. G., et al. Neurofibromatosis 2 tumour suppressor schwannomin interacts with betaII-spectrin. *Nat Genet.* 1998;18(4):354-9.

80. Kimura Y., Koga H., Araki N., Mugita N., Fujita N., et al. The involvement of calpain-dependent proteolysis of the tumor suppressor NF2 (merlin) in schwannomas and meningiomas. *Nat Med.* 1998;4(8):915-22.

81. Asthagiri A. R., Parry D. M., Butman J. A., Kim H. J., Tsilou E. T., et al. Neurofibromatosis type 2. *Lancet.* 2009;373(9679):1974-86.

82. Evans D. G. Neurofibromatosis type 2 (NF2): a clinical and molecular review. *Orphanet J Rare Dis.* 2009;4(16.

83. Seizinger B. R., Martuza R. L., and Gusella J. F. Loss of genes on chromosome 22 in tumorigenesis of human acoustic neuroma. *Nature.* 1986;322(6080):644-7.

84. Goutagny S., and Kalamarides M. Meningiomas and neurofibromatosis. *J Neurooncol.* 2010;99(3):341-7.

85. Evans D. G., Huson S. M., Donnai D., Neary W., Blair V., et al. A clinical study of type 2 neurofibromatosis. *Q J Med.* 1992;84(304):603-18.

86. Evans D. G., Watson C., King A., Wallace A. J., and Baser M. E. Multiple meningiomas: differential involvement of the NF2 gene in children and adults. *J Med Genet.* 2005;42(1):45-8.

87. Evans D. G., Birch J. M., and Ramsden R. T. Paediatric presentation of type 2 neurofibromatosis. *Arch Dis Child.* 1999;81(6):496-9.

88. Perry A., Giannini C., Raghavan R., Scheithauer B. W., Banerjee R., et al. Aggressive phenotypic and genotypic features in pediatric and NF2-associated meningiomas: a clinicopathologic study of 53 cases. *J Neuropathol Exp Neurol.* 2001;60(10):994-1003.

89. Eaton K. W., Tooke L. S., Wainwright L. M., Judkins A. R., and Biegel J. A. Spectrum of SMARCB1/INI1 mutations in familial and sporadic rhabdoid tumors. *Pediatr Blood Cancer.* 2011;56(1):7-15.

90. Sevenet N., Sheridan E., Amram D., Schneider P., Handgretinger R., et al. Constitutional mutations of the hSNF5/INI1 gene predispose to a variety of cancers. *Am J Hum Genet.* 1999;65(5):1342-8.

91. Taylor M. D., Gokgoz N., Andrulis I. L., Mainprize T. G., Drake J. M., et al. Familial posterior fossa brain tumors of infancy secondary to germline mutation of the hSNF5 gene. *Am J Hum Genet.* 2000;66(4):1403-6.

92. Versteege I., Sevenet N., Lange J., Rousseau-Merck M. F., Ambros P., et al. Truncating mutations of hSNF5/INI1 in aggressive paediatric cancer. *Nature.* 1998;394(6689):203-6.

93. Boyd C., Smith M. J., Kluwe L., Balogh A., Maccollin M., et al. Alterations in the SMARCB1 (INI1) tumor suppressor gene in familial schwannomatosis. *Clin Genet.* 2008;74(4):358-66.

94. Hadfield K. D., Newman W. G., Bowers N. L., Wallace A., Bolger C., et al. Molecular characterisation of SMARCB1 and NF2 in familial and sporadic schwannomatosis. *J Med Genet.* 2008;45(6):332-9.

95. Hulsebos T. J., Kenter S. B., Jakobs M. E., Baas F., Chong B., et al. SMARCB1/INI1 maternal germ line mosaicism in schwannomatosis. *Clin Genet.* 2010;77(1):86-91.

96. Smith M. J., Wallace A. J., Bowers N. L., Rustad C. F., Woods C. G., et al. Frequency of SMARCB1 mutations in familial and sporadic schwannomatosis. *Neurogenetics.* 2012;13(2):141-5.

97. Bacci C., Sestini R., Provenzano A., Paganini I., Mancini I., et al. Schwannomatosis associated with multiple meningiomas due to a familial SMARCB1 mutation. *Neurogenetics.* 2010;11(1):73-80.

98. Christiaans I., Kenter S. B., Brink H. C., van Os T. A., Baas F., et al. Germline SMARCB1 mutation and somatic NF2 mutations in familial multiple meningiomas. *J Med Genet.* 2011;48(2):93-7.

99. van den Munckhof P., Christiaans I., Kenter S. B., Baas F., and Hulsebos T. J. Germline SMARCB1 mutation predisposes to multiple meningiomas and schwannomas with preferential location of cranial meningiomas at the falx cerebri. *Neurogenetics.* 2012;13(1):1-7.

100. Harada T., Irving R. M., Xuereb J. H., Barton D. E., Hardy D. G., et al. Molecular genetic investigation of the neurofibromatosis type 2 tumor suppressor gene in sporadic meningioma. *J Neurosurg.* 1996;84(5):847-51.

101. Clark V. E., Erson-Omay E. Z., Serin A., Yin J., Cotney J., et al. Genomic analysis of non-NF2 meningiomas reveals mutations in TRAF7, KLF4, AKT1, and SMO. *Science.* 2013;339(6123):1077-80.

102. Gutmann D. H., Giordano M. J., Fishback A. S., and Guha A. Loss of merlin expression in sporadic meningiomas, ependymomas and schwannomas. *Neurology.* 1997;49(1):267-70.

103. Ruttledge M. H., Sarrazin J., Rangaratnam S., Phelan C. M., Twist E., et al. Evidence for the complete inactivation of the NF2 gene in the majority of sporadic meningiomas. *Nat Genet.* 1994;6(2):180-4.

104. Lamszus K., Kluwe L., Matschke J., Meissner H., Laas R., et al. Allelic losses at 1p, 9q, 10q, 14q, and 22q in the progression of aggressive meningiomas and undifferentiated meningeal sarcomas. *Cancer Genet Cytogenet.* 1999;110(2):103-10.

105. Ozaki S., Nishizaki T., Ito H., and Sasaki K. Comparative genomic hybridization analysis of genetic alterations associated with malignant progression of meningioma. *J Neurooncol.* 1999;41(2):167-74.

106. Perry A., Gutmann D. H., and Reifenberger G. Molecular pathogenesis of meningiomas. *J Neurooncol.* 2004;70(2):183-202.

107. Weber R. G., Bostrom J., Wolter M., Baudis M., Collins V. P., et al. Analysis of genomic alterations in benign, atypical, and anaplastic meningiomas: toward

a genetic model of meningioma progression. *Proc Natl Acad Sci U S A.* 1997;94(26):14719-24.

108. Brastianos P. K., Horowitz P. M., Santagata S., Jones R. T., McKenna A., et al. Genomic sequencing of meningiomas identifies oncogenic SMO and AKT1 mutations. *Nat Genet.* 2013;45(3):285-9.

109. Reuss D. E., Piro R. M., Jones D. T., Simon M., Ketter R., et al. Secretory meningiomas are defined by combined KLF4 K409Q and TRAF7 mutations. *Acta Neuropathol.* 2013;125(3):351-8.

110. Scudiero I., Zotti T., Ferravante A., Vessichelli M., Reale C., et al. Tumor necrosis factor (TNF) receptor-associated factor 7 is required for TNFalpha-induced Jun NH2-terminal kinase activation and promotes cell death by regulating polyubiquitination and lysosomal degradation of c-FLIP protein. *J Biol Chem.* 2012;287(8):6053-61.

111. Takahashi K., Tanabe K., Ohnuki M., Narita M., Ichisaka T., et al. Induction of pluripotent stem cells from adult human fibroblasts by defined factors. *Cell.* 2007;131(5):861-72.

112. Vivanco I., and Sawyers C. L. The phosphatidylinositol 3-Kinase AKT pathway in human cancer. *Nat Rev Cancer.* 2002;2(7):489-501.

113. Taipale J., Chen J. K., Cooper M. K., Wang B., Mann R. K., et al. Effects of oncogenic mutations in Smoothened and Patched can be reversed by cyclopamine. *Nature.* 2000;406(6799):1005-9.

114. Taipale J., and Beachy P. A. The Hedgehog and Wnt signalling pathways in cancer. *Nature.* 2001;411(6835):349-54.

115. Rieske P., Zakrzewska M., Piaskowski S., Jaskolski D., Sikorska B., et al. Molecular heterogeneity of meningioma with INI1 mutation. *Mol Pathol.* 2003;56(5):299-301.

116. Schmitz U., Mueller W., Weber M., Sevenet N., Delattre O., et al. INI1 mutations in meningiomas at a potential hotspot in exon 9. *Br J Cancer.* 2001;84(2):199-201.

117. Morozov A., Yung E., and Kalpana G. V. Structure-function analysis of integrase interactor 1/hSNF5L1 reveals differential properties of two repeat motifs present in the highly conserved region. *Proc Natl Acad Sci U S A.* 1998;95(3):1120-5.

118. Phelan M. L., Sif S., Narlikar G. J., and Kingston R. E. Reconstitution of a core chromatin remodeling complex from SWI/SNF subunits. *Mol Cell.* 1999;3(2):247-53.

119. Cairns B. R., Kim Y. J., Sayre M. H., Laurent B. C., and Kornberg R. D. A multisubunit complex containing the SWI1/ADR6, SWI2/SNF2, SWI3, SNF5, and SNF6 gene products isolated from yeast. *Proc Natl Acad Sci U S A.* 1994;91(5):1950-4.

120. Cote J., Quinn J., Workman J. L., and Peterson C. L. Stimulation of GAL4 derivative binding to nucleosomal DNA by the yeast SWI/SNF complex. *Science.* 1994;265(5168):53-60.

121. Wilson B. G., and Roberts C. W. SWI/SNF nucleosome remodellers and cancer. *Nat Rev Cancer.* 2011;11(7):481-92.

122. Kornberg R. D. Chromatin structure: a repeating unit of histones and DNA. *Science.* 1974;184(4139):868-71.

123. Saha A., Wittmeyer J., and Cairns B. R. Chromatin remodelling: the industrial revolution of DNA around histones. *Nat Rev Mol Cell Biol.* 2006;7(6):437-47.

124. Lorch Y., Maier-Davis B., and Kornberg R. D. Mechanism of chromatin remodeling. *Proc Natl Acad Sci U S A.* 2010;107(8):3458-62.

125. Oruetxebarria I., Venturini F., Kekarainen T., Houweling A., Zuijderduijn L. M., et al. P16INK4a is required for hSNF5 chromatin remodeler-induced cellular senescence in malignant rhabdoid tumor cells. *J Biol Chem.* 2004;279(5):3807-16.

126. John S., Sabo P. J., Johnson T. A., Sung M. H., Biddie S. C., et al. Interaction of the glucocorticoid receptor with the chromatin landscape. *Mol Cell.* 2008;29(5):611-24.

127. Chai B., Huang J., Cairns B. R., and Laurent B. C. Distinct roles for the RSC and Swi/Snf ATP-dependent chromatin remodelers in DNA double-strand break repair. *Genes Dev.* 2005;19(14):1656-61.

128. Gong F., Fahy D., and Smerdon M. J. Rad4-Rad23 interaction with SWI/SNF links ATP-dependent chromatin remodeling with nucleotide excision repair. *Nat Struct Mol Biol.* 2006;13(10):902-7.

129. Lee H. S., Park J. H., Kim S. J., Kwon S. J., and Kwon J. A cooperative activation loop among SWI/SNF, gamma-H2AX and H3 acetylation for DNA double-strand break repair. *Embo j.* 2010;29(8):1434-45.

130. Flanagan J. F., and Peterson C. L. A role for the yeast SWI/SNF complex in DNA replication. *Nucleic Acids Res.* 1999;27(9):2022-8.

131. Sawa H., Kouike H., and Okano H. Components of the SWI/SNF complex are required for asymmetric cell division in C. elegans. *Mol Cell.* 2000;6(3):617-24.

132. Xue Y., Canman J. C., Lee C. S., Nie Z., Yang D., et al. The human SWI/SNF-B chromatin-remodeling complex is related to yeast rsc and localizes at kinetochores of mitotic chromosomes. *Proc Natl Acad Sci U S A.* 2000;97(24):13015-20.

133. Zhang H. S., Gavin M., Dahiya A., Postigo A. A., Ma D., et al. Exit from G1 and S phase of the cell cycle is regulated by repressor complexes containing HDAC-Rb-hSWI/SNF and Rb-hSWI/SNF. *Cell.* 2000;101(1):79-89.

134. de la Serna I. L., Ohkawa Y., and Imbalzano A. N. Chromatin remodelling in mammalian differentiation: lessons from ATP-dependent remodellers. *Nat Rev Genet.* 2006;7(6):461-73.

135. Flowers S., Nagl N. G., Jr., Beck G. R., Jr., and Moran E. Antagonistic roles for BRM and BRG1 SWI/SNF complexes in differentiation. *J Biol Chem.* 2009;284(15):10067-75.

136. Lessard J., Wu J. I., Ranish J. A., Wan M., Winslow M. M., et al. An essential switch in subunit composition of a chromatin remodeling complex during neural development. *Neuron.* 2007;55(2):201-15.

137. Young D. W., Pratap J., Javed A., Weiner B., Ohkawa Y., et al. SWI/SNF chromatin remodeling complex is obligatory for BMP2-induced, Runx2-dependent skeletal gene expression that controls osteoblast differentiation. *J Cell Biochem.* 2005;94(4):720-30.

138. Gao X., Tate P., Hu P., Tjian R., Skarnes W. C., et al. ES cell pluripotency and germ-layer formation require the SWI/SNF chromatin remodeling component BAF250a. *Proc Natl Acad Sci U S A.* 2008;105(18):6656-61.

139. Shain A. H., and Pollack J. R. The spectrum of SWI/SNF mutations, ubiquitous in human cancers. *PLoS One.* 2013;8(1):e55119.

140. Varela I., Tarpey P., Raine K., Huang D., Ong C. K., et al. Exome sequencing identifies frequent mutation of the SWI/SNF complex gene PBRM1 in renal carcinoma. *Nature.* 2011;469(7331):539-42.

141. Shain A. H., Giacomini C. P., Matsukuma K., Karikari C. A., Bashyam M. D., et al. Convergent structural alterations define SWItch/Sucrose NonFermentable (SWI/SNF) chromatin remodeler as a central tumor suppressive complex in pancreatic cancer. *Proc Natl Acad Sci U S A.* 2012;109(5):E252-9.

142. Wong A. K., Shanahan F., Chen Y., Lian L., Ha P., et al. BRG1, a component of the SWI-SNF complex, is mutated in multiple human tumor cell lines. *Cancer Res.* 2000;60(21):6171-7.

143. Li M., Zhao H., Zhang X., Wood L. D., Anders R. A., et al. Inactivating mutations of the chromatin remodeling gene ARID2 in hepatocellular carcinoma. *Nat Genet.* 2011;43(9):828-9.

144. Bochar D. A., Wang L., Beniya H., Kinev A., Xue Y., et al. BRCA1 is associated with a human SWI/SNF-related complex: linking chromatin remodeling to breast cancer. *Cell.* 2000;102(2):257-65.

145. Drost J., Mantovani F., Tocco F., Elkon R., Comel A., et al. BRD7 is a candidate tumour suppressor gene required for p53 function. *Nat Cell Biol.* 2010;12(4):380-9.

146. Huang J., Zhao Y. L., Li Y., Fletcher J. A., and Xiao S. Genomic and functional evidence for an ARID1A tumor suppressor role. *Genes Chromosomes Cancer.* 2007;46(8):745-50.

147. Xia W., Nagase S., Montia A. G., Kalachikov S. M., Keniry M., et al. BAF180 is a critical regulator of p21 induction and a tumor suppressor mutated in breast cancer. *Cancer Res.* 2008;68(6):1667-74.

148. Jones S., Wang T. L., Shih Ie M., Mao T. L., Nakayama K., et al. Frequent mutations of chromatin remodeling gene ARID1A in ovarian clear cell carcinoma. *Science.* 2010;330(6001):228-31.

149. Wiegand K. C., Shah S. P., Al-Agha O. M., Zhao Y., Tse K., et al. ARID1A mutations in endometriosis-associated ovarian carcinomas. 2010;363(16):1532-43.

150. Fukuoka J., Fujii T., Shih J. H., Dracheva T., Meerzaman D., et al. Chromatin remodeling factors and BRM/BRG1 expression as prognostic indicators in non-small cell lung cancer. *Clin Cancer Res.* 2004;10(13):4314-24.

151. Medina P. P., Carretero J., Fraga M. F., Esteller M., Sidransky D., et al. Genetic and epigenetic screening for gene alterations of the chromatin-remodeling factor, SMARCA4/BRG1, in lung tumors. *Genes Chromosomes Cancer.* 2004;41(2):170-7.

152. Reisman D. N., Sciarrotta J., Wang W., Funkhouser W. K., and Weissman B. E. Loss of BRG1/BRM in human lung cancer cell lines and primary lung cancers: correlation with poor prognosis. *Cancer Res.* 2003;63(3):560-6.

153. Rodriguez-Nieto S., Canada A., Pros E., Pinto A. I., Torres-Lanzas J., et al. Massive parallel DNA pyrosequencing analysis of the tumor suppressor

BRG1/SMARCA4 in lung primary tumors. *Hum Mutat.* 2011;32(2):E1999-2017.

154. Parsons D. W., Li M., Zhang X., Jones S., Leary R. J., et al. The genetic landscape of the childhood cancer medulloblastoma. *Science.* 2011;331(6016):435-9.

155. Jackson E. M., Sievert A. J., Gai X., Hakonarson H., Judkins A. R., et al. Genomic analysis using high-density single nucleotide polymorphism-based oligonucleotide arrays and multiplex ligation-dependent probe amplification provides a comprehensive analysis of INI1/SMARCB1 in malignant rhabdoid tumors. *Clin Cancer Res.* 2009;15(6):1923-30.

156. Biegel J. A., Zhou J. Y., Rorke L. B., Stenstrom C., Wainwright L. M., et al. Germ-line and acquired mutations of INI1 in atypical teratoid and rhabdoid tumors. *Cancer Res.* 1999;59(1):74-9.

157. Modena P., Lualdi E., Facchinetti F., Galli L., Teixeira M. R., et al. SMARCB1/INI1 tumor suppressor gene is frequently inactivated in epithelioid sarcomas. *Cancer Res.* 2005;65(10):4012-9.

158. Mobley B. C., McKenney J. K., Bangs C. D., Callahan K., Yeom K. W., et al. Loss of SMARCB1/INI1 expression in poorly differentiated chordomas. *Acta Neuropathol.* 2010;120(6):745-53.

159. Guidi C. J., Sands A. T., Zambrowicz B. P., Turner T. K., Demers D. A., et al. Disruption of Ini1 leads to peri-implantation lethality and tumorigenesis in mice. *Mol Cell Biol.* 2001;21(10):3598-603.

160. Klochendler-Yeivin A., Fiette L., Barra J., Muchardt C., Babinet C., et al. The murine SNF5/INI1 chromatin remodeling factor is essential for embryonic development and tumor suppression. *EMBO Rep.* 2000;1(6):500-6.

161. Roberts C. W., Galusha S. A., McMenamin M. E., Fletcher C. D., and Orkin S. H. Haploinsufficiency of Snf5 (integrase interactor 1) predisposes to malignant rhabdoid tumors in mice. *Proc Natl Acad Sci U S A.* 2000;97(25):13796-800.

162. Roberts C. W., Leroux M. M., Fleming M. D., and Orkin S. H. Highly penetrant, rapid tumorigenesis through conditional inversion of the tumor suppressor gene Snf5. *Cancer Cell.* 2002;2(5):415-25.

163. Isakoff M. S., Sansam C. G., Tamayo P., Subramanian A., Evans J. A., et al. Inactivation of the Snf5 tumor suppressor stimulates cell cycle progression and cooperates with p53 loss in oncogenic transformation. *Proc Natl Acad Sci U S A.* 2005;102(49):17745-50.

164. Nobori T., Miura K., Wu D. J., Lois A., Takabayashi K., et al. Deletions of the cyclin-dependent kinase-4 inhibitor gene in multiple human cancers. *Nature.* 1994;368(6473):753-6.

165. McKenna E. S., Sansam C. G., Cho Y. J., Greulich H., Evans J. A., et al. Loss of the epigenetic tumor suppressor SNF5 leads to cancer without genomic instability. *Mol Cell Biol.* 2008;28(20):6223-33.

166. Zhang Z. K., Davies K. P., Allen J., Zhu L., Pestell R. G., et al. Cell cycle arrest and repression of cyclin D1 transcription by INI1/hSNF5. *Mol Cell Biol.* 2002;22(16):5975-88.

167. Alarcon-Vargas D., Zhang Z., Agarwal B., Challagulla K., Mani S., et al. Targeting cyclin D1, a downstream effector of INI1/hSNF5, in rhabdoid tumors. *Oncogene.* 2006;25(5):722-34.

168. Smith M. E., Cimica V., Chinni S., Jana S., Koba W., et al. Therapeutically targeting cyclin D1 in primary tumors arising from loss of Ini1. *Proc Natl Acad Sci U S A.* 2011;108(1):319-24.

169. Lunenburger H., Lanvers-Kaminsky C., Lechtape B., and Fruhwald M. C. Systematic analysis of the antiproliferative effects of novel and standard anticancer agents in rhabdoid tumor cell lines. *Anticancer Drugs.* 2010;21(5):514-22.

170. Hanahan D., and Weinberg R. A. The hallmarks of cancer. *Cell.* 2000;100(1):57-70.

171. Meyer N., and Penn L. Z. Reflecting on 25 years with MYC. *Nat Rev Cancer.* 2008;8(12):976-90.

172. Nagl N. G., Jr., Zweitzig D. R., Thimmapaya B., Beck G. R., Jr., and Moran E. The c-myc gene is a direct target of mammalian SWI/SNF-related complexes during differentiation-associated cell cycle arrest. *Cancer Res.* 2006;66(3):1289-93.

173. Gadd S., Sredni S. T., Huang C. C., and Perlman E. J. Rhabdoid tumor: gene expression clues to pathogenesis and potential therapeutic targets. *Lab Invest.* 2010;90(5):724-38.

174. Ingham P. W., and McMahon A. P. Hedgehog signaling in animal development: paradigms and principles. *Genes Dev.* 2001;15(23):3059-87.

175. Varjosalo M., and Taipale J. Hedgehog: functions and mechanisms. *Genes Dev.* 2008;22(18):2454-72.

176. Roessler E., Belloni E., Gaudenz K., Jay P., Berta P., et al. Mutations in the human Sonic Hedgehog gene cause holoprosencephaly. *Nat Genet.* 1996;14(3):357-60.

177. Rubin L. L., and de Sauvage F. J. Targeting the Hedgehog pathway in cancer. *Nat Rev Drug Discov.* 2006;5(12):1026-33.

178. Hahn H., Wicking C., Zaphiropoulous P. G., Gailani M. R., Shanley S., et al. Mutations of the human homolog of Drosophila patched in the nevoid basal cell carcinoma syndrome. *Cell.* 1996;85(6):841-51.

179. Johnson R. L., Rothman A. L., Xie J., Goodrich L. V., Bare J. W., et al. Human homolog of patched, a candidate gene for the basal cell nevus syndrome. *Science.* 1996;272(5268):1668-71.

180. Reifenberger J., Wolter M., Weber R. G., Megahed M., Ruzicka T., et al. Missense mutations in SMOH in sporadic basal cell carcinomas of the skin and primitive neuroectodermal tumors of the central nervous system. *Cancer Res.* 1998;58(9):1798-803.

181. Xie J., Murone M., Luoh S. M., Ryan A., Gu Q., et al. Activating Smoothened mutations in sporadic basal-cell carcinoma. *Nature.* 1998;391(6662):90-2.

182. Taylor M. D., Liu L., Raffel C., Hui C. C., Mainprize T. G., et al. Mutations in SUFU predispose to medulloblastoma. *Nat Genet.* 2002;31(3):306-10.

183. Jagani Z., Mora-Blanco E. L., Sansam C. G., McKenna E. S., Wilson B., et al. Loss of the tumor suppressor Snf5 leads to aberrant activation of the Hedgehog-Gli pathway. *Nat Med.* 2010;16(12):1429-33.

184. Dahmane N., Lee J., Robins P., Heller P., and Ruiz i Altaba A. Activation of the transcription factor Gli1 and the Sonic hedgehog signalling pathway in skin tumours. *Nature.* 1997;389(6653):876-81.

185. Unden A. B., Zaphiropoulos P. G., Bruce K., Toftgard R., and Stahle-Backdahl M. Human patched (PTCH) mRNA is overexpressed consistently in tumor cells of both familial and sporadic basal cell carcinoma. *Cancer Res.* 1997;57(12):2336-40.

186. Bird A. Perceptions of epigenetics. *Nature.* 2007;447(7143):396-8.

187. Jones P. A., and Baylin S. B. The fundamental role of epigenetic events in cancer. *Nat Rev Genet.* 2002;3(6):415-28.

188. Bracken A. P., and Helin K. Polycomb group proteins: navigators of lineage pathways led astray in cancer. *Nat Rev Cancer.* 2009;9(11):773-84.

189. Cao R., Wang L., Wang H., Xia L., Erdjument-Bromage H., et al. Role of histone H3 lysine 27 methylation in Polycomb-group silencing. *Science.* 2002;298(5595):1039-43.

190. Kennison J. A. The Polycomb and trithorax group proteins of Drosophila: trans-regulators of homeotic gene function. *Annu Rev Genet.* 1995;29(289-303.

191. Kia S. K., Gorski M. M., Giannakopoulos S., and Verrijzer C. P. SWI/SNF mediates polycomb eviction and epigenetic reprogramming of the INK4b-ARF-INK4a locus. *Mol Cell Biol.* 2008;28(10):3457-64.

192. Ramirez-Carrozzi V. R., Braas D., Bhatt D. M., Cheng C. S., Hong C., et al. A unifying model for the selective regulation of inducible transcription by CpG islands and nucleosome remodeling. *Cell.* 2009;138(1):114-28.

193. Shao Z., Raible F., Mollaaghababa R., Guyon J. R., Wu C. T., et al. Stabilization of chromatin structure by PRC1, a Polycomb complex. *Cell.* 1999;98(1):37-46.

194. Wilson B. G., Wang X., Shen X., McKenna E. S., Lemieux M. E., et al. Epigenetic antagonism between polycomb and SWI/SNF complexes during oncogenic transformation. *Cancer Cell.* 2010;18(4):316-28.

195. Simon J. A., and Lange C. A. Roles of the EZH2 histone methyltransferase in cancer epigenetics. *Mutat Res.* 2008;647(1-2):21-9.

196. Choi M., Scholl U. I., Ji W., Liu T., Tikhonova I. R., et al. Genetic diagnosis by whole exome capture and massively parallel DNA sequencing. *Proc Natl Acad Sci U S A.* 2009;106(45):19096-101.

197. Lunter G., and Goodson M. Stampy: a statistical algorithm for sensitive and fast mapping of Illumina sequence reads. *Genome Res.* 2011;21(6):936-9.

198. Li H., and Durbin R. Fast and accurate short read alignment with Burrows-Wheeler transform. *Bioinformatics.* 2009;25(14):1754-60.

199. DePristo M. A., Banks E., Poplin R., Garimella K. V., Maguire J. R., et al. A framework for variation discovery and genotyping using next-generation DNA sequencing data. *Nat Genet.* 2011;43(5):491-8.

200. O'Roak B. J., Vives L., Fu W., Egertson J. D., Stanaway I. B., et al. Multiplex targeted sequencing identifies recurrently mutated genes in autism spectrum disorders. *Science.* 2012;338(6114):1619-22.

201. Olshen A. B., Venkatraman E. S., Lucito R., and Wigler M. Circular binary segmentation for the analysis of array-based DNA copy number data. *Biostatistics.* 2004;5(4):557-72.

202. Huttner W. B., Gerdes H. H., and Rosa P. The granin (chromogranin/secretogranin) family. *Trends Biochem Sci.* 1991;16(1):27-30.

203. Ozawa H., and Takata K. The granin family--its role in sorting and secretory granule formation. *Cell Struct Funct.* 1995;20(6):415-20.

204. Kirchmair R., Hogue-Angeletti R., Gutierrez J., Fischer-Colbrie R., and Winkler H. Secretoneurin--a neuropeptide generated in brain, adrenal medulla and other endocrine tissues by proteolytic processing of secretogranin II (chromogranin C). *Neuroscience.* 1993;53(2):359-65.

205. Courel M., El Yamani F. Z., Alexandre D., El Fatemi H., Delestre C., et al. Secretogranin II is overexpressed in advanced prostate cancer and promotes the neuroendocrine differentiation of prostate cancer cells. *Eur J Cancer.* 2014;50(17):3039-49.

206. Shyu W. C., Lin S. Z., Chiang M. F., Chen D. C., Su C. Y., et al. Secretoneurin promotes neuroprotection and neuronal plasticity via the Jak2/Stat3 pathway in murine models of stroke. *J Clin Invest.* 2008;118(1):133-48.

207. Kim K. A., Zhao J., Andarmani S., Kakitani M., Oshima T., et al. R-Spondin proteins: a novel link to beta-catenin activation. *Cell Cycle.* 2006;5(1):23-6.

208. Seshagiri S., Stawiski E. W., Durinck S., Modrusan Z., Storm E. E., et al. Recurrent R-spondin fusions in colon cancer. *Nature.* 2012;488(7413):660-4.

209. Gong X., Yi J., Carmon K. S., Crumbley C. A., Xiong W., et al. Aberrant RSPO3-LGR4 signaling in Keap1-deficient lung adenocarcinomas promotes tumor aggressiveness. *Oncogene.* 2014.

210. Martin J. L., and Baxter R. C. Insulin-like growth factor-binding protein from human plasma. Purification and characterization. *J Biol Chem.* 1986;261(19):8754-60.

211. Takaoka M., Smith C. E., Mashiba M. K., Okawa T., Andl C. D., et al. EGF-mediated regulation of IGFBP-3 determines esophageal epithelial cellular response to IGF-I. *Am J Physiol Gastrointest Liver Physiol.* 2006;290(2):G404-16.

212. Chang Y. S., Wang L., Liu D., Mao L., Hong W. K., et al. Correlation between insulin-like growth factor-binding protein-3 promoter methylation and prognosis of patients with stage I non-small cell lung cancer. *Clin Cancer Res.* 2002;8(12):3669-75.

213. Figueroa J. A., De Raad S., Tadlock L., Speights V. O., and Rinehart J. J. Differential expression of insulin-like growth factor binding proteins in high versus low Gleason score prostate cancer. *J Urol.* 1998;159(4):1379-83.

214. Hanafusa T., Yumoto Y., Nouso K., Nakatsukasa H., Onishi T., et al. Reduced expression of insulin-like growth factor binding protein-3 and its promoter hypermethylation in human hepatocellular carcinoma. *Cancer Lett.* 2002;176(2):149-58.